

Successor Features Support Model-based and Model-free Reinforcement Learning

Lucas Lehnert

*Computer Science Department
Brown University
Providence, RI 02912, USA*

LUCAS.LEHNERT@BROWN.EDU

Michael L. Littman

*Computer Science Department
Brown University
Providence, RI 02912, USA*

MICHAEL.LITTMAN@BROWN.EDU

Abstract

One key challenge in reinforcement learning is the ability to generalize knowledge in control problems. While deep learning methods have been successfully combined with model-free reinforcement-learning algorithms, how to perform model-based reinforcement learning in the presence of approximation errors still remains an open problem. Using successor features, a feature representation that predicts a temporal constraint, this paper presents three contributions: First, it shows how learning successor features is equivalent to model-free learning. Then, it shows how successor features encode model reductions that compress the state space by creating state partitions of bisimilar states. Using this representation, an intelligent agent is guaranteed to accurately predict future reward outcomes, a key property of model-based reinforcement-learning algorithms. Lastly, it presents a loss objective and prediction error bounds showing that accurately predicting value functions and reward sequences is possible with an approximation of successor features. On finite control problems, we illustrate how minimizing this loss objective results in approximate bisimulations. The results presented in this paper provide a novel understanding of representations that can support model-free and model-based reinforcement learning.

Keywords: Reinforcement Learning, Feature Representations, Model Reductions, Bisimulation Relations, Linear Action Models

1. Introduction

Research in reinforcement learning (RL) (Sutton and Barto, 1998; Kaelbling et al., 1996) devises algorithms for computing an action-selection strategy, also called a *policy*, that maximizes a reward objective in a control problem. In a control problem, also called an *environment*, an agent uses its policy to choose an action at the current state to cause a transition between states and generate a reward, a single scalar number. One key assumption—Markovianity—states that rewards and transitions depend only on the current state but are otherwise assumed to be arbitrary. RL algorithms can be coarsely classified into model-free algorithms or model-based algorithms. Model-free RL algorithms arrive at an optimal policy through continued trial-and-error interactions with the control problem while simultaneously improving an intermediate policy (Watkins and Dayan, 1992; Rummery, 1995; Mnih et al., 2013), perhaps indirectly through value estimates. Model-based RL algorithms

estimate the transition and reward function and use this learned model to compute the optimal policy (Sutton, 1990; Brafman and Tenenbholz, 2002). While algorithms such as Dyna (Sutton, 1990) also use model-free TD-learning, this paper considers a “strict” form of model-based RL where the optimal policy is computed explicitly from a learned model, rather than using a model to speed up or inform otherwise model-free learning. One shortcoming of model-based RL is that approximation errors of a single-step transition model compound for predictions over multiple time steps. At each time step, the transition model only outputs an approximate state, and this approximate state is then re-used to predict the state for the next time step. As a result, the predicted state sequence diverges from the true state sequence as the number of time steps increase (Talvitie, 2017). Further, a predicted state sequence may not contain actual states, rendering the prediction of future reward outcomes difficult.

Dayan (1993) presents the successor representation (SR), a representation that encodes each state in terms of the visitation frequencies over future states. The SR has also been extended to successor features (SFs) (Barreto et al., 2017; Lehnert et al., 2017) by first encoding the state into a feature vector and then estimating SFs to predict visitation frequencies over future states. Because the SR encodes future state visitation frequencies, the SR also encodes information about the transition dynamics of a control problem and can be seen as an intermediate between model-based and model-free RL algorithms (Momennejad et al., 2017; Russek et al., 2017).

In this paper, we present a novel perspective on how SFs relate to model-free and model-based RL. First, we show that learning SFs is equivalent to learning value functions directly from trial-and-error interactions with the environment. Hence, learning SFs is akin model-free RL. Then, we show that if SFs are used to learn a state representation, then this state representation encodes a compression of the transition and reward function, also called a model reduction (Givan et al., 2003). Rather than just representing one control policy that can be improved, model reductions, and thus SFs, encode a representation of the control task itself, a key property of model-based RL algorithms. This approach provides a novel perspective on model-based RL: Rather than finding approximations of the one-step transition and reward function, a state representation is learned that compresses the dynamics of a control task into a linear action model (Yao and Szepesvári, 2012). Because the state space is compressed using a model reduction, the linear action model is guaranteed to produce the same reward sequences as the original control problem given any arbitrary action sequence. If no approximation errors are present, the linear action model will simulate reward sequences in the same way as the original control problem. If approximation errors are present, the learned linear action model resembles a “softened” model reduction and produces reward sequences that approximately resemble reward sequences produced by the original control problem. For this case we present prediction errors bounds linear in the objective function used to train the model.

2. State Representations in Reinforcement Learning

A *Markov decision process (MDP)* is a tuple $M = \langle \mathcal{S}, \mathcal{A}, p, r, \gamma \rangle$, with a state space \mathcal{S} , a action space \mathcal{A} , a transition function $p(s, a, s') = \Pr\{s'|s, a\}$, a reward function $r : \mathcal{S} \times \mathcal{A} \times \mathcal{S} \rightarrow \mathbb{R}$, and a discount factor $\gamma \in [0, 1)$. For finite state and action spaces, the transition

and reward functions can also be written in matrix or vector notation as a left-stochastic state-to-state transition matrix \mathbf{P}^a and an expected reward vector \mathbf{r}^a of dimension $|\mathcal{S}|$. Each entry of \mathbf{r}^a is set to $\mathbb{E}_{s'}[r(s, a, s')|s, a]$, where the expectation is computed over next states s' . This paper will consider both finite (“discrete”) or uncountably infinite (“continuous”) state spaces.

A policy $\pi : \mathcal{S} \times \mathcal{A} \rightarrow [0, 1]$ specifies the probabilities with which actions are selected at any given state (and $\sum_{a \in \mathcal{A}} \pi(s, a) = 1$). If a policy π is used, the transition function and expected rewards generated by this policy are denoted by \mathbf{P}^π and \mathbf{r}^π , respectively. The value function

$$V^\pi(s) = \mathbb{E}_\pi \left[\sum_{t=1}^{\infty} \gamma^{t-1} r(s_t, a_t, s_{t+1}) \middle| s_0 = s \right] \quad (1)$$

predicts the expected discounted return where the expectation is computed over all infinite length trajectories that start in state s and select actions according to the policy π . The value function V^π can also be written as a vector $\mathbf{v}^\pi = \sum_{t=1}^{\infty} \gamma^{t-1} (\mathbf{P}^\pi)^{t-1} \mathbf{r}^\pi$. The action-conditional Q-function is defined similarly as

$$Q^\pi(s, a) = \mathbb{E}_\pi \left[\sum_{t=1}^{\infty} \gamma^{t-1} r(s_t, a_t, s_{t+1}) \middle| s_1 = s, a_1 = a \right] \quad (2)$$

$$= r(s, a) + \gamma \mathbb{E}_{s'} [V^\pi(s')], \quad (3)$$

where Eq. (3) is the usual Bellman fixed point (Puterman, 1994). The expectation in Eq. (2) ranges over all infinite length trajectories generated by a policy π but that start at state s with action a . The expected reward is denoted with $r(s, a)$. A *basis function* (Sutton, 1996; Konidaris et al., 2011) is a function mapping states s or state-action pairs (s, a) to a real valued vector. Specifically, a *state-conditional* basis function maps a state s to a column vector $\boldsymbol{\phi}_s$, and a *state-action-conditional* basis function maps a state-action pair to a column vector $\boldsymbol{\xi}_{s,a}$. Basis functions perform transforms on the state or state-action space to be able to represent a certain objective effectively, for example, to express linear approximations of the Q-function with

$$Q(s, a) \approx \boldsymbol{\xi}_{s,a}^\top \boldsymbol{\theta}. \quad (4)$$

For finite action spaces, state-conditional basis functions can be used to construct a state-action-conditional basis function by constructing a feature vector of dimension $|\mathcal{A}| \cdot \dim \boldsymbol{\phi}_s^1$ and placing the vector $\boldsymbol{\phi}_s$ into the entries corresponding to action a and setting all other entries to zero. Specifically, for each state s ,

$$\boldsymbol{\xi}_{s,a_1} = [\boldsymbol{\phi}_s^\top, \mathbf{0}, \dots, \mathbf{0}]^\top, \quad (5)$$

$$\boldsymbol{\xi}_{s,a_2} = [\mathbf{0}, \boldsymbol{\phi}_s^\top, \dots, \mathbf{0}]^\top, \quad (6)$$

$$\vdots \quad (7)$$

$$\boldsymbol{\xi}_{s,a_n} = [\mathbf{0}, \dots, \mathbf{0}, \boldsymbol{\phi}_s^\top]^\top. \quad (8)$$

1. The dimension of the vector $\boldsymbol{\phi}_s$ is denoted with $\dim \boldsymbol{\phi}_s$.

Dayan (1993) introduced the successor representation (SR), a feature representation for finite state and action spaces that predicts visitation frequencies over future states. Suppose each state s in a finite state space is written as a one-hot vector \mathbf{s} of dimension $|\mathcal{S}|$, then for any fixed policy π the SR is defined as $\psi^\pi(s) = \mathbb{E} [\sum_{t=1}^{\infty} \gamma^{t-1} \mathbf{s}_t | \mathbf{s}_0 = \mathbf{s}]^2$. In matrix notation, a SR for a particular policy π can be written as

$$\Psi_{\text{SR}}^\pi = \sum_{t=1}^{\infty} \gamma^{t-1} (\mathbf{P}^\pi)^{t-1}. \quad (9)$$

Intuitively, the matrix Ψ_{SR}^π describes a discounted visitation frequency of all future states. A column of $(1 - \gamma)\Psi_{\text{SR}}^\pi$ then contains a marginal probability (over time steps) of reaching a specific state, where the number of time steps needed to reach a state follows a geometric distribution with parameter γ . Similar to value functions, the SR obeys a recursive identity

$$\Psi_{\text{SR}}^a = \mathbf{I} + \gamma \mathbf{P}^a \Psi_{\text{SR}}^\pi, \quad (10)$$

where Ψ_{SR}^a has a dependency on the policy π (Lehnert et al., 2017). Barreto et al. (2017) generalize the SR to successor features (SFs) by assuming that state-action pairs are represented with a basis function ξ . The SF at state s for selecting action a is defined as

$$\psi_{s,a}^\pi = \mathbb{E}_\pi \left[\sum_{t=0}^{\infty} \gamma^{t-1} \xi_{s_t, a_t} \middle| s_0 = s, a_0 = a \right], \quad (11)$$

where the expectation ranges over all infinite length trajectories generated by a policy π but that start at state s with action a . SFs and the SR are closely tied to value functions. If the expected rewards $r(s, a)$ are written out in a vector

$$\mathbf{w} = [r(s_1, a_1), \dots, r(s_n, a_m)]^\top, \quad (12)$$

then the expected reward function can be parametrized using \mathbf{w} and the one-hot bit vector (state-action-conditioned) basis function $\mathbf{e}_{s,a}$ with

$$r(s, a) = \mathbf{e}_{s,a}^\top \mathbf{w}. \quad (13)$$

With this parametrization of the reward function, substituting Eq. (13) into Eq. (2) shows that SFs form an exact basis function for Q-values (Barreto et al., 2017):

$$\begin{aligned} Q^\pi(s, a) &= \mathbb{E}_\pi \left[\sum_{t=1}^{\infty} \gamma^{t-1} r(s_t, a_t) \middle| s_0 = s, a_0 = a \right] \\ &= \mathbb{E}_\pi \left[\sum_{t=1}^{\infty} \gamma^{t-1} \mathbf{e}_{s_t, a_t}^\top \mathbf{w} \middle| s_0 = s, a_0 = a \right] \\ &= \mathbb{E}_\pi \left[\sum_{t=1}^{\infty} \gamma^{t-1} \mathbf{e}_{s_t, a_t} \middle| s_0 = s, a_0 = a \right]^\top \mathbf{w} \\ &= (\psi_{s,a}^\pi)^\top \mathbf{w}. \end{aligned} \quad (14)$$

A similar connection holds between state-conditional value functions V^π and the SR.

2. Rather than writing the SR using an indicator function, we use one-hot bit vectors \mathbf{s} , which is equivalent.

3. Model-Free Learning

Because SFs are linear in the value function, algorithms that learn SFs can be derived similarly to linear Q-learning (Sutton and Barto, 1998, Chapter 8.4). In linear Q-learning, stochastic gradient descent is used to optimize the Mean Squared Value Error

$$\text{VE}(\boldsymbol{\theta}) = \sum_{s,a,r,s'} \mu(s,a,r,s') \left(Q_{\boldsymbol{\theta}}^{\pi}(s,a) - y_{r,s'} \right)^2, \quad (15)$$

where $Q_{\boldsymbol{\theta}}^{\pi}(s,a) = \boldsymbol{\xi}_{s,a}^{\top} \boldsymbol{\theta}$ and $y_{r,s'} = r + \gamma \max_{a'} Q_{\boldsymbol{\theta}}^{\pi}(s',a')$. The expectation in Eq. (15) is computed with respect to some distribution μ with which transitions (s,a,r,s') are sampled. When computing a gradient of $\text{VE}(\boldsymbol{\theta})$ the *target* $y_{r,s'}$ is considered a constant. For each transition (s,a,r,s') , linear Q-learning performs the update rule

$$\boldsymbol{\theta}_{t+1} = \boldsymbol{\theta}_t + \alpha_Q \underbrace{\left(r + \gamma \max_{a'} Q_{\boldsymbol{\theta}}^{\pi}(s',a') - Q_{\boldsymbol{\theta}}^{\pi}(s,a) \right)}_{=\delta} \boldsymbol{\xi}_{s,a}, \quad (16)$$

where α_Q is a learning rate. The term δ is called the TD-error. Similar to Lehnert et al. (2017), an SF-learning algorithm can be derived by defining the Mean Squared SF Error

$$\text{SFE}(\boldsymbol{\psi}^{\pi}) = \sum_{s,a,r,s'} \mu(s,a,r,s') \|\boldsymbol{\psi}_{s,a}^{\pi} - \mathbf{y}_{s,a,r,s'}\|^2. \quad (17)$$

Because the SF $\boldsymbol{\psi}_{s,a}^{\pi}$ is a vector of dimension n , the target

$$\mathbf{y}_{s,a,r,s'} = \boldsymbol{\xi}_{s,a} + \gamma \boldsymbol{\psi}_{s',a^*}^{\pi} \quad (18)$$

is also a vector of dimension n . The action a^* selected at the next time step is computed greedily with respect to the Q-value estimate:

$$a^* = \arg \max_a \left(\boldsymbol{\psi}_{s',a}^{\pi} \right)^{\top} \mathbf{w}, \quad (19)$$

where the weight vector \mathbf{w} is the reward model parameter vector from Eq. (13). We make the assumption that SFs are approximated linearly using the basis function $\boldsymbol{\xi}$ and that

$$\boldsymbol{\psi}_{s,a}^{\pi} = \mathbf{F} \boldsymbol{\xi}_{s,a}, \quad (20)$$

where \mathbf{F} is a square matrix. Computing the gradient of $\text{SFE}(\boldsymbol{\psi}^{\pi})$ with respect to \mathbf{F} results in an update rule similar to linear Q-learning:

$$\mathbf{F}_{t+1} = \mathbf{F}_t + \alpha_{\psi} \underbrace{\left(\boldsymbol{\xi}_{s,a} + \gamma \boldsymbol{\psi}_{s',a^*}^{\pi} - \boldsymbol{\psi}_{s,a}^{\pi} \right)}_{=\delta_{\psi}} \boldsymbol{\xi}_{s,a}^{\top}. \quad (21)$$

We call the error term δ_{ψ} the *SF-error*. The iterate in Eq. (21) is similar the TD update rules presented by Dayan (1993); Barreto et al. (2017); Lehnert et al. (2017). Similarly, the reward model is optimized using the loss objective $\sum_{s,a,r,s'} \mu(s,a,r,s') \left(\boldsymbol{\xi}_{s,a}^{\top} \mathbf{w} - r(s,a) \right)^2$ resulting in the update rule

$$\mathbf{w}_{t+1} = \mathbf{w}_t + \alpha_r \left(\boldsymbol{\xi}_{s,a}^{\top} \mathbf{w}_t - r(s,a) \right) \boldsymbol{\xi}_{s,a}. \quad (22)$$

Algorithm 1 SF-learning

```

1: loop
2:   Collect transition  $(s, a, r, s')$  using control policy  $\pi$ .
3:    $a^* = \arg \max_{a'} \left( \psi_{s',a'}^\pi \right)^\top \mathbf{w}_t$ 
4:    $\mathbf{F}_{t+1} = \mathbf{F}_t + \alpha_\psi \left( \xi_{s,a} + \gamma \mathbf{F}_t \xi_{s',a^*} - \mathbf{F}_t \xi_{s,a} \right) \xi_{s,a}^\top$ 
5:    $\mathbf{w}_{t+1} = \mathbf{w}_t + \alpha_r \left( \xi_{s,a}^\top \mathbf{w}_t - r(s, a) \right) \xi_{s,a}$ 
6: end loop

```

Algorithm 1 summarizes the algorithm, which we refer to as *SF-learning*.

Both linear Q-learning and SF-learning are off-policy learning algorithms, because a control policy η is used to select actions while the value function of a different optimal policy π is learned. Suppose $\eta : s, Q(s, \cdot), t \mapsto a$ is a function of the state s and the Q-value estimates $Q(s, \cdot)$ at state s , and the time step t . For example, ε -greedy exploration represents such a policy, because with ε probability the action greedy with respect to the current Q-value estimates is selected. Further, the parameter ε could be annealed to zero as the time step t increases. For this class of control policies, linear Q-learning and SF-learning produce the same sequence of value functions, assuming that SF-learning is provided with an optimal reward model.

Theorem 1 (SF-learning and Q-learning Equivalence). *Consider an MDP $M = \langle \mathcal{S}, \mathcal{A}, p, r, \gamma \rangle$ and a basis function ξ such that*

$$\forall s, a, \xi_{s,a}^\top \mathbf{w} = r(s, a). \quad (23)$$

Suppose linear Q-learning and SF-learning are run in M starting at state s_{start} using a control policy $\eta : s, Q(s, \cdot), t \mapsto a$. If $\alpha_\psi = \alpha_Q$, $\mathbf{w}_0 = \mathbf{w}$, and $\mathbf{w}^\top \mathbf{F}_0 = \boldsymbol{\theta}_0^\top$, then

$$\forall t \geq 0, \mathbf{w}^\top \mathbf{F}_t = \boldsymbol{\theta}_t^\top. \quad (24)$$

As a result, linear Q-learning and SF-learning will produce the same Q-value function sequence and trajectory.

Appendix A presents a formal proof of Theorem 1. Note that this result also applies to fixed control policies η that do not change with the time step or the current value estimates—the policy η can depend on a state s , Q-values, and time step t , but does not have to. If both algorithms produce the same sequence of value functions up to time step t , then they will choose the same actions with equal probabilities for the next time step. If SF-learning is not initialized with the correct reward weight vector \mathbf{w} and is required to learn a reward model, then both algorithms will not produce identical value function sequences and behaviour. Theorem 1 points out the key distinction between SF-learning and Q-learning: Q-learning samples the reward function directly by incorporating the reward of each transition directly into its Q-value estimates while SF-learning first builds a reward model. However, if the reward model is initialized to the correct “ground truth” reward function, SF-learning becomes identical to Q-learning and—most importantly—searches for the optimal policy in the same fashion. In this light, learning SFs is akin to model-free RL.

4. Successor Features Encode Model-based Representations

The previous section shows how learning SFs is closely related to learning value functions from temporal difference errors, given a fixed basis function. In this section the learning problem is changed by including the basis function into the set of parameters the agent aims to learn. Specifically, state-conditional basis functions are considered that can produce accurate SFs and one step reward predictions. We will show that these two criteria are sufficient to characterize and learn a feature representation that resembles a model reduction. Section 4.1 reviews model reductions and Section 4.2 presents how SFs can be related to model reductions. Section 4.3 shows how model reductions can be approximated by learning SFs and Section 4.4 presents two experiments on finite state-action MDPs to illustrate how model reductions can be approximated using gradient-based optimization techniques.

4.1 Model Reductions

A model reduction (Givan et al., 2003) is a partitioning of the state space \mathcal{S} such that two states of the same partition are equivalent in terms of their on step rewards as well as states reachable within one time step. The example grid world shown in Figure 1 illustrates the intuition behind model reductions. In this MDP, each column forms a state partition because two criteria are satisfied:

1. the one-step rewards are the same, and
2. for two states of the same partition, the distributions over next state partitions are identical.

The compressed MDP retains all information necessary to predict future reward outcomes, because the columns describe the distance in terms of time steps to the +1 reward. For example, suppose a model-based agent is in the left (blue) column and wants to predict the reward sequence when moving right twice. If the state space is partitioned as shown in Figure 1(a), then the agent can predict the correct reward sequence 0, 0, 1 using only state clusters. If the blue and green column were merged into one partition, then the agent will not be able to predict the correct reward sequence. In that case the state space is compressed into two partitions and the information about the distance to the right column is lost. Consequently an agent placed into the left column and moving right could not distinguish if the +1 reward occurs in one or two time steps using only the transitions and rewards between state partitions. States that are merged into the same partition by a model reduction are called *behaviourally equivalent* or *bisimilar*.

Bisimilarity can be formally defined as an equivalence relation between different states, which induces a partitioning of the state space. The set of state partitions are formally defined as follows.

Definition 1 (Quotient/Partition Set). *Let \mathcal{S} be a set and \sim an equivalence relation defined on \mathcal{S} . Then, the quotient or partition set*

$$\mathcal{S} / \sim \stackrel{\text{def.}}{=} \{[s] | \forall s, s' \in [s], s \sim s'\}. \quad (25)$$

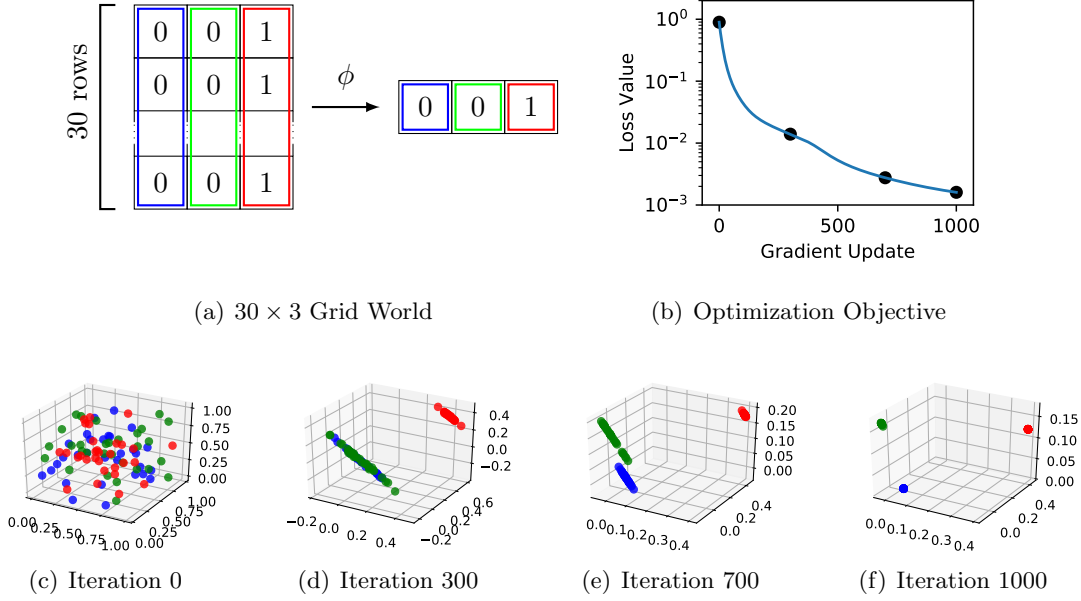


Figure 1: Model features in the column grid world example (similar to “upworld” (Abel et al., 2017)). The agent can move up, down, left, or right, and will always receive a +1 reward for selecting an action in the red column, and a zero reward otherwise. Model reductions collapse each column into a single state (right grid in 1(a)). This three-state MDP captures all relevant dynamics: the +1 reward state is distinct from the remaining states, which describe the distance to the positive reward state. The row index is not needed for evaluating an arbitrary policy or for predicting reward sequences. Our goal is to optimize an initially random feature representation (Figure 1(c)) so that bisimilar states are assigned approximately the same feature vector (Figure 1(f)). We accomplish this by using a SF model to construct a loss objective and minimizing this objective using gradient descent (Figure 1(b)). The dots in Figure 1(b) correspond to the different feature representations shown in Figure 1(c) through 1(f) obtained during training.

Each element $[s] \in \mathcal{S}/\sim$ is a state partition, a subset of the state space, and \mathcal{S}/\sim is a set of partitions. Bisimilarity can be formally defined as follows.

Definition 2 (Bisimilarity). *For an MDP $M = \langle \mathcal{S}, \mathcal{A}, p, r, \gamma \rangle$, where $p(s, a, \cdot) : \mathcal{S} \rightarrow [0, 1]$ is either a probability distribution over states if \mathcal{S} is discrete or a density function if \mathcal{S} is continuous. The equivalence relation \sim^b is a bisimulation if,*

$$s \sim^b \tilde{s} \iff \forall a \in \mathcal{A}, r(s, a) = r(\tilde{s}, a) \text{ and } \forall \phi \in \mathcal{S}/\sim^b, Pr\{s \xrightarrow{a} \phi\} = Pr\{\tilde{s} \xrightarrow{a} \phi\}, \quad (26)$$

where for discrete state spaces \mathcal{S} ,

$$Pr\{s \xrightarrow{a} \phi\} = \sum_{s' \in \phi} p(s, a, s'), \quad (27)$$

and for continuous state spaces \mathcal{S} ,

$$Pr\{s \xrightarrow{a} \phi\} = \int_{s' \in \phi} p(s, a, s') ds'. \quad (28)$$

The condition (26) states that two states can only be bisimilar if they produce the same one-step rewards and if they transition to the same partition with the same probability. Note that this condition on the transition dynamics is recursive: Two bisimilar states s and \tilde{s} have to transition with equal probability to a partition ϕ , that itself can only consist of bisimilar states. For discrete state spaces, Definition 2 is identical to the definition presented by Li et al. (2006). For continuous state spaces Eq. (28) generalizes the same idea by integrating the transition function over the state partition ϕ .

4.2 Connection to Successor Features

As discussed before, a state-conditional basis function ϕ maps states into some feature space and thus establishes a many-to-one relation between states and features. Model reductions can be encoded through a basis function by constraining ϕ such that two states can only be assigned the same feature vector if they are bisimilar. For example, the feature representation ϕ could be constructed by partitioning the state space into n partitions and then assigning each partition a unique n dimensional one-hot bit vector. We introduce *model features*, which assign identical feature vectors to states that are bisimilar.

Definition 3 (Model Features). *A feature representation $\phi : \mathcal{S} \rightarrow \mathbb{R}^n$ is a model feature if and only if*

$$\forall s, \tilde{s} : \phi_s = \phi_{\tilde{s}} \implies s \sim^b \tilde{s}. \quad (29)$$

Because of their relationship to bisimulation, model features are designed to be rich enough to allow the prediction of future reward outcomes while removing any other information from the state space. Note that in contrast to Abel et al. (2018), the work presented in this paper does not attempt to compute a maximal compression of the state space. Hence, if states are encoded as one-hot bit vectors then the identity map provides a trivial model feature for finite state spaces (each partition consist of a singleton set).

Suppose $\phi : \mathcal{S} \rightarrow \{\mathbf{e}_1, \dots, \mathbf{e}_n\}$ is a feature representation and \mathbf{e}_i is a one-hot bit vector of dimension n with the i th entry being set to 1. In that case, the representation ϕ partitions the state space by assigning the same one-hot bit vector to states of the same partition. Implicitly the function ϕ encodes an equivalence relation $\overset{\phi}{\sim}$ such that

$$\forall s, \tilde{s} : \phi_s = \phi_{\tilde{s}} \iff s \overset{\phi}{\sim} \tilde{s}. \quad (30)$$

Definition 2 states that a bisimulation relation can only relate states with equal one step expected rewards. Suppose $\phi : \mathcal{S} \rightarrow \{\mathbf{e}_1, \dots, \mathbf{e}_n\}$ is such that

$$\forall s, \forall a, r(s, a) = \phi_s^\top \mathbf{r}_\phi^a, \quad (31)$$

then each entry of the vector \mathbf{r}_ϕ^a contains the expected reward value associated with a particular state partition and action because ϕ_s is a one-hot bit vector. Thus we have that

$$\forall s, \tilde{s}, \forall a \in \mathcal{A} : s \overset{\phi}{\sim} \tilde{s} \implies r(s, a) = r(\tilde{s}, a), \quad (32)$$

because both s and \tilde{s} are assigned the same feature vector. If ϕ satisfies Eq. (31), then the resulting equivalence relation $\overset{\phi}{\sim}$ satisfies the reward condition in Definition 2.

SFs encode the condition on the transition dynamics of bisimulation relations. For two states s and \tilde{s} to be bisimilar, they have to transition to the same state partition with equal probability. Repeating from Definition 2, the state space needs to be partitioned such that for any such two states s and \tilde{s} ,

$$\forall a \in \mathcal{A}, \phi' \in \mathcal{S} / \overset{b}{\sim}, \Pr \left\{ s \overset{a}{\rightarrow} \phi' \right\} = \Pr \left\{ \tilde{s} \overset{a}{\rightarrow} \phi' \right\}. \quad (33)$$

The probability $\Pr \left\{ s \overset{a}{\rightarrow} \phi' \right\}$ describes the marginal of transitioning from a state s into any state that lies in the state partition labelled with the vector ϕ' . To relate these probabilities to SFs, we first observe that the probability of transitioning from partition to partition can be written as the marginal

$$\Pr \left\{ \phi \overset{a}{\rightarrow} \phi' \middle| \omega \right\} = \int_{s \in \phi} \omega(s) \Pr \left\{ s \overset{a}{\rightarrow} \phi' \right\} ds, \quad (34)$$

where ω is the probability of encountering a state s in the state partition ϕ . The distribution ω can be understood as a visitation distribution over states generated by a particular policy. This paper refers to ω as a weighting function.

Definition 4 (Weighting Function). *For an MDP $M = \langle \mathcal{S}, \mathcal{A}, p, r, \gamma \rangle$, let \sim be an equivalence relation on the state space \mathcal{S} . If \mathcal{S} is discrete, then the weighting function $\omega : \mathcal{S} \rightarrow [0, 1]$ is defined such that*

$$\forall \phi \in \mathcal{S} / \sim, \sum_{s \in \phi} \omega(s) = 1. \quad (35)$$

If \mathcal{S} is continuous, then the weighting function $\omega : \mathcal{S} \rightarrow [0, 1]$ is defined such that

$$\forall \phi \in \mathcal{S} / \sim, \int_{s \in \phi} \omega(s) ds = 1. \quad (36)$$

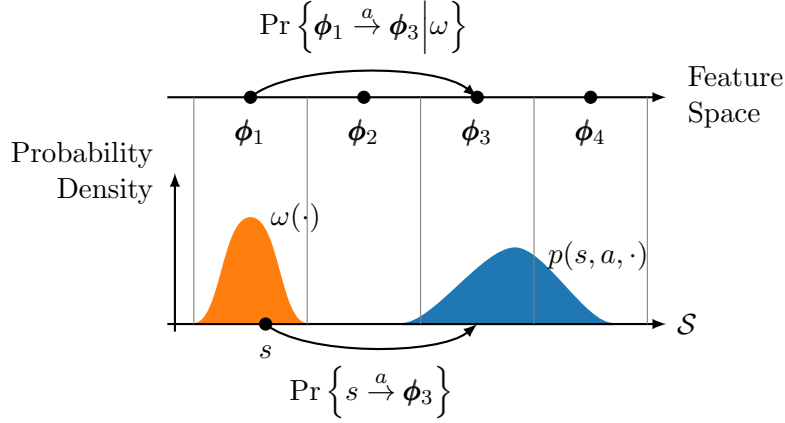


Figure 2: Weighting functions determine partition-to-partition transition probabilities. Suppose the state space \mathcal{S} is a bounded interval in \mathbb{R} and a feature representation clusters states into four partitions as shown above. Each partition is labelled with one feature vector from the set $\{\phi_1, \phi_2, \phi_3, \phi_4\}$. The schematic plots the density function p over states of selecting action a at state s (blue area) and the density function ω over the state partition ϕ_1 (orange area). The probability of transitioning to the partition ϕ_3 is denoted with $\Pr\{s \xrightarrow{a} \phi_3\}$ and the probability of transitioning from partition-to-partition is denoted with $\Pr\{\phi_1 \xrightarrow{a} \phi_3 | \omega\}$. If a transition (s, a, s') is mapped to a transition (ϕ_1, a, ϕ_3) , then the probability with which this transition in feature space occurs depends on the probability with which states are sampled from the partition ϕ_1 . The weighting function ω models this probability distribution.

Figure 2 shows a schematic of how the different probability distributions relate to one another. Suppose we define the SF

$$\boldsymbol{\psi}^{\bar{\pi}}(s, a) = \boldsymbol{\phi}_s^\top \mathbf{F}^a \text{ and } \boldsymbol{\phi}_s^\top \mathbf{F}^a = \boldsymbol{\phi}_s^\top + \gamma \mathbb{E}_{\bar{\pi}} \left[\boldsymbol{\phi}_{s'}^\top \mathbf{F}^{\bar{\pi}} \middle| s, a \right], \quad (37)$$

then each row \mathbf{F}^a contains the SF associated with all states belonging to the same partition. The right hand side of the fix-point equation in line (37) computes the expected SF across all actions a with respect to a policy $\bar{\pi}$:

$$\mathbb{E}_{\bar{\pi}} [\boldsymbol{\psi}^{\bar{\pi}}(s, a) | s] = \sum_a \pi(s, a) \boldsymbol{\phi}_s^\top \mathbf{F}^a = \boldsymbol{\phi}_s^\top \underbrace{\left(\sum_a \text{diag}\{\pi(\mathbf{e}_i, a)\}_{i=1}^n \mathbf{F}^a \right)}_{=\mathbf{F}^{\bar{\pi}}}, \quad (38)$$

where $\text{diag}\{\pi(\mathbf{e}_i, a)\}_{i=1}^n$ is $n \times n$ matrix with the action-selection probabilities along its diagonal. This dependency of the SF representation on $\bar{\pi}$ will be discussed at the end of this section.

Because $\boldsymbol{\phi}_s$ is a one-hot bit vector, we can construct a partition-to-partition transition matrix $\mathbf{P}_{\phi, \omega}^a$ such that

$$\mathbf{P}_{\phi, \omega}^a(i, j) = \Pr \left\{ \mathbf{e}_i \xrightarrow{a} \mathbf{e}_j \middle| \omega \right\}. \quad (39)$$

Leveraging the property that $\boldsymbol{\phi}_s$ is a one-hot bit vector, the matrix \mathbf{F}^a encodes the visitation frequencies over state partitions, similar to how the SR matrix $\boldsymbol{\Psi}_{\text{SR}}^a$ encodes the visitation frequencies over states. This property stems from the fact that $\boldsymbol{\psi}^{\bar{\pi}}$ is a function of the feature representation $\boldsymbol{\phi}$. Previously we have shown that $\boldsymbol{\Psi}_{\text{SR}}^a = \mathbf{I} + \gamma \mathbf{P}^a \boldsymbol{\Psi}_{\text{SR}}^{\bar{\pi}}$ (see also Eq. (10)) and similarly we can write for each matrix $\{\mathbf{F}^a\}_a$

$$\mathbf{F}^a = \mathbf{I} + \gamma \mathbf{P}_{\phi, \omega}^a \mathbf{F}^{\bar{\pi}}. \quad (40)$$

Interestingly, because the matrices $\{\mathbf{F}^a\}_a$ are used to compute a SF with respect to the transition dynamics of the MDP, the feature representation $\boldsymbol{\phi}$ is constructed such that

$$\forall \omega, \omega', \forall a \in \mathcal{A}, \mathbf{P}_{\phi, \omega}^a = \mathbf{P}_{\phi, \omega'}^a. \quad (41)$$

Eq. (41) implies that we could pick for any state s a weighting function ω that is a Dirac delta function centered around s and

$$\Pr \left\{ \boldsymbol{\phi} \xrightarrow{a} \boldsymbol{\phi}' \middle| \omega \right\} = \int_{s \in \boldsymbol{\phi}} \omega(s) \Pr \left\{ s \xrightarrow{a} \boldsymbol{\phi}' \right\} ds = \Pr \left\{ s \xrightarrow{a} \boldsymbol{\phi}' \right\}. \quad (42)$$

Meaning two states s and \tilde{s} of the same state partition $\boldsymbol{\phi}$ will transition to state partitions with equal probability and $\Pr \left\{ s \xrightarrow{a} \boldsymbol{\phi}' \right\} = \Pr \left\{ \tilde{s} \xrightarrow{a} \boldsymbol{\phi}' \right\}$. To see why the partition-to-partition transition probabilities become independent of ω , we observe that the SF $\boldsymbol{\psi}^{\bar{\pi}}(s, a)$ describes the visitation frequencies over future state partitions. If two states s and \tilde{s} are assigned to the same partition, then $\boldsymbol{\psi}^{\bar{\pi}}(s, a) = \boldsymbol{\psi}^{\bar{\pi}}(\tilde{s}, a)$ for every action a . That is, both states s and \tilde{s} must have identical future state-partition visitation frequencies and thus $\Pr \left\{ s \xrightarrow{a} \boldsymbol{\phi}' \right\} = \Pr \left\{ \tilde{s} \xrightarrow{a} \boldsymbol{\phi}' \right\}$. Because these state-to-partition transition probabilities are equal for all states of the same partition, the integral in Eq. (42) evaluates to the same value for any ω . The following lemma proves lines (41) and (42) formally.

Lemma 1. *For an MDP $M = \langle \mathcal{S}, \mathcal{A}, p, r, \gamma \rangle$, let $\phi : \mathcal{S} \rightarrow \{\mathbf{e}_1, \dots, \mathbf{e}_n\}$ be a feature representation and \mathbf{e}_i be a one-hot bit vector of dimension n with entry i being set to 1. If*

$$\forall s \in \mathcal{S}, \forall a \in \mathcal{A}, \phi_s^\top \mathbf{F}^a = \phi_s^\top + \gamma \mathbb{E} \left[\phi_{s'}^\top \mathbf{F}^\pi \middle| s, a \right], \quad (43)$$

then

1. $\exists \{\mathbf{P}_\phi^a\}_a : \mathbf{F}^a = \mathbf{I} + \gamma \mathbf{P}_\phi^a \mathbf{F}^\pi$ where \mathbf{P}_ϕ^a is a left-stochastic matrix, and
2. $\forall \omega, \omega', \mathbf{P}_{\phi, \omega}^a = \mathbf{P}_{\phi, \omega'}^a = \mathbf{P}_\phi^a$, where ω and ω' are arbitrary weighting functions.

Appendix A presents a formal proof of Lemma 1. Using this lemma and the previously presented arguments, we can prove the main theorem which shows that SFs and a one-step reward predictor are sufficient to construct model features and thus model reductions.

Theorem 2. *For an MDP $M = \langle \mathcal{S}, \mathcal{A}, p, r, \gamma \rangle$, let $\phi : \mathcal{S} \rightarrow \{\mathbf{e}_1, \dots, \mathbf{e}_n\}$ be a feature representation and \mathbf{e}_i be a one-hot bit vector of dimension n with the i th entry being set to 1. If the feature representation ϕ satisfies for some exploratory policy $\bar{\pi}$ that*

$$\forall s \in \mathcal{S}, \forall a \in \mathcal{A}, r(s, a) = \phi_s^\top \mathbf{r}_\phi^a \text{ and } \phi_s^\top \mathbf{F}^a = \phi_s^\top + \gamma \mathbb{E} \left[\phi_{s'}^\top \mathbf{F}^\pi \middle| s, a \right], \quad (44)$$

then ϕ is a model-feature and any two states s and \tilde{s} are bisimilar if $\phi_s = \phi_{\tilde{s}}$.

A formal proof of Theorem 2 is listed in Appendix A. The SF

$$\psi^\pi(s, a) = \mathbb{E} \left[\sum_{t=1}^{\infty} \gamma^{t-1} \phi_s \middle| s, a, \bar{\pi} \right] \quad (45)$$

is action-conditional, meaning the SF depends on the policy $\bar{\pi}$ after the first time step because the expectation in Eq. (45) ranges over all trajectories that start at state s with action a —action a is not selected according to $\bar{\pi}$. This dependency of the first time step on an action is sufficient to encode the state-to-partition transition probabilities in the matrices $\{\mathbf{F}^a\}_a$. Because the feature representation ϕ is conditioned only on the state and is constrained to predict action-conditional SFs, it is independent of the policy $\bar{\pi}$. In fact, any exploratory policy $\bar{\pi}$ can be used to construct SFs and model features. By Lemma 1, the partition-to-partition transition probabilities can be computed analytically with³

$$\mathbf{P}_\phi^a = \frac{1}{\gamma} (\mathbf{F}^a - \mathbf{I}) (\mathbf{F}^\pi)^{-1}. \quad (46)$$

If a one-hot bit vector feature representation can be constructed satisfying the conditions outlined in Theorem 2, then in principle any policy $\bar{\pi}$ could be used to construct model features. However, if model features are approximated then a dependency on $\bar{\pi}$ becomes visible to some extent. The following sections explore how model features can be approximated and illustrate that in the presence of approximation errors a model feature approximation produces weaker predictions for policies that are increasingly dissimilar to $\bar{\pi}$.

3. The proof of Lemma 1 in Appendix A shows formally why the inverse of \mathbf{F}^π exists.

4.3 Approximate Model Reductions

This section will generalize the previously discussed model to arbitrary basis functions $\phi : \mathcal{S} \rightarrow \mathbb{R}^n$ and show how model features can be approximated. Rather than reasoning about approximate bisimulations in the form of bisimulation metrics (Ferns et al., 2011, 2004), we will consider two key properties to characterize approximations of model features:

1. the ability to predict reward sequences given any arbitrary start state and action sequence, and
2. the ability to predict the value function of any arbitrary policy π .

We will present our results for arbitrary state spaces and introduce two small values ε_r and ε_ψ we desire to minimize:

$$\forall s \in \mathcal{S}, \forall a \in \mathcal{A}, \left| \phi_s^\top \mathbf{r}_\phi^a - r(s, a) \right| \leq \varepsilon_r, \quad (47)$$

$$\text{and } \left\| \phi_s^\top + \gamma \mathbb{E}_{s'} \left[\phi_{s'}^\top \mathbf{F}^\pi \middle| s, a \right] - \phi_s^\top \mathbf{F}^a \right\|_2 \leq \varepsilon_\psi, \quad (48)$$

where the following assumption is made about the matrices $\{\mathbf{F}^a\}_a$:

Assumption 1. *Assume that for every action a , there exists a matrix \mathbf{P}_ϕ^a with $\|\mathbf{P}_\phi^a\|_2 \leq 1$ such that $\mathbf{F}^a = \mathbf{I} + \gamma \mathbf{P}_\phi^a \mathbf{F}^\pi$.*

In contrast to the one-hot bit vector model discussed previously, Assumption 1 is required because for any arbitrary feature representation it may not be possible to predict the feature-to-feature transitions linearly. While the following results are stated for finite action spaces, they can also be extended to arbitrary action spaces by assuming functions $r_\phi : a \mapsto \mathbf{r}_\phi^a$ rather than a set of vectors $\{\mathbf{r}_\phi^a\}_a$ and similarly for the matrices $\{\mathbf{F}^a\}_a$.

4.3.1 ROLLOUT PREDICTIONS

Given a start state s , the expected future reward after selecting actions according to the sequence a_1, \dots, a_T can be approximated with

$$\mathbb{E}[r_T | s, a_1, \dots, a_T] \approx \phi_s^\top \mathbf{P}_\phi^{a_1} \dots \mathbf{P}_\phi^{a_{T-1}} \mathbf{r}_\phi^{a_T}, \quad (49)$$

where the expectation is over all possible T -step trajectories starting in s and following the given action sequence a_1, \dots, a_T .

Theorem 3 (Rollout Bound). *Consider an MDP $M = \langle \mathcal{S}, \mathcal{A}, p, r, \gamma \rangle$ and assume that ε_r and ε_ψ are defined as in Eq. (47) and Eq. (48), then $\forall T \geq 1, s, a_1, \dots, a_T$,*

$$\left| \phi_s^\top \mathbf{P}_\phi^{a_1} \dots \mathbf{P}_\phi^{a_{T-1}} \mathbf{r}_\phi^{a_T} - \mathbb{E}_{s'}[r_T | s, a_1, \dots, a_T] \right| \leq \varepsilon_r + \frac{(T-1)(1-\gamma)}{\gamma} \varepsilon_\psi \max_a \|\mathbf{r}_\phi^a\|_2. \quad (50)$$

If $T = 1$, then the bound in Eq. (50) is equal to ε_r because the transition model is not used to predict one-step rewards and cannot influence the prediction error. SF predict visitation frequencies over future transitions and are thus discounted multi-step models. Because a multi-step model is used for multi-step predictions, the second term in Eq. (50),

which describes the prediction error induced due to approximation errors in the transition model, is linear in ε_ψ and the rollout length T .

This result stands in contrast to the usual approach of approximating a one-step transition model. The drawback of directly approximating transition functions is that approximation errors compound when making multi-step predictions, because predictions about the state at time step $t+1$ are made given only an approximation of the state at time step t . Hence, existing error bounds are exponential in T (Asadi et al., 2018, Theorem 1) (Talvitie, 2017, Lemma 2). This dependency does not appear in Theorem 3 because ε_ψ directly upper bounds a discounted multi-step transition model. Our model is free to construct any feature space that produces low prediction errors. Hence, if ε_ψ is low enough, then Theorem 3 shows that the learned feature space can support predictions about multi-step transitions.

4.3.2 VALUE PREDICTIONS

The following theorem states that an approximation of model features can also be used to represent Q-value functions such that $Q^\pi(s, a) \approx \phi_s^\top \mathbf{q}_\phi^a$ for every action a . Because value functions are a discounted sum of expected future rewards, the ability of model features to be suitable for Q-value prediction follows from the previous discussion.

Theorem 4 (Approximate Model Features). *Consider an MDP $M = \langle \mathcal{S}, \mathcal{A}, p, r, \gamma \rangle$ and assume that ε_r and ε_ψ are defined as in Eq. (47) and Eq. (48), then*

$$\forall \pi, s, a, \quad \left| Q^\pi(s, a) - \phi_s^\top \mathbf{q}_\phi^a \right| \leq \frac{\varepsilon_r}{1-\gamma} + \frac{\varepsilon_\psi (1+\gamma)}{(1-\gamma)^2} \max_a \|\mathbf{r}_\phi^a\|_2, \quad (51)$$

The value error bound Eq. (51) is also linear in ε_ψ and, similarly to the rollout bound in Eq. (50), this linear dependency stems from the fact that ε_ψ bounds the prediction error of a discounted multi-step model. Note that if approximation errors are very high, then both error bounds in Theorem 3 and Theorem 4 can grow to a value larger than the reward or possible value range of the MDP at hand.

4.4 Learning Model Features

Using the previously presented results, model features, and thus model reductions, can be approximated via (stochastic) gradient descent on the loss objective

$$\mathcal{L}(\phi, \{\mathbf{F}^a\}_a, \{\mathbf{r}_\phi^a\}_a) = \mathbb{E} \left[\left(\phi_s^\top \mathbf{r}_\phi^a - r(s, a) \right)^2 + \alpha \left\| \phi_s^\top + \gamma \phi_s^\top \mathbf{F}^\pi - \phi_s^\top \mathbf{F}^a \right\|_2^2 \right], \quad (52)$$

where the expectation ranges over all possible transitions that are sampled as training data. For all experiments we assume π to select actions uniformly at random. The gradient of \mathcal{L} is computed with respect to all parameters $\phi, \{\mathbf{F}^a\}_a, \{\mathbf{r}_\phi^a\}_a$, and ϕ could be any arbitrary function parametrized by some weight vector. The experiments presented in this section focus on finite state and action spaces, hence

$$\phi_s = \mathbf{s} \Phi, \quad (53)$$

where \mathbf{s} is a one-hot bit vector representation of the state s , and Φ is a real valued matrix. For stochastic gradient descent a transition data set is collected and each gradient update is computed by sampling a (sub)set of transitions from the entire transition data set.

To access how well a learned feature representation can be used to predict the value function of an arbitrary policy, we fix a particular policy π that is defined on the state space \mathcal{S} and record the value error $\|\Phi \mathbf{v}_\phi^\pi - \mathbf{v}^\pi\|_\infty$ for each policy π . Note that for estimating \mathbf{v}_ϕ^π , only the feature transition and reward models $\{\mathbf{P}_\phi^a\}_a$ and $\{\mathbf{r}_\phi^a\}_a$ are used. The state-conditional value function $V^\pi(s)$ can be expressed as a vector

$$\mathbf{v}^\pi = \sum_a \Pi^a \mathbf{q}^a \quad (54)$$

where $\Pi^a = \text{diag}\{\pi(s, a)\}_s$. Algorithm 2 outlines how \mathbf{v}_ϕ^π is computed, which is similar to performing value iteration but with a fixed policy defined in the original state space \mathcal{S} . Line 2 in Algorithm 2 first computes the value function $\mathbf{v}^\pi = \sum_a \Pi^a \Phi \mathbf{q}_\phi^a$, which is defined on the original state space \mathcal{S} because each entry of the vector \mathbf{v}^π corresponds to the value $V^\pi(s)$ of some state s . The pseudo inverse Φ^+ is used to solve the equation $\Phi \mathbf{v}_\phi^\pi = \mathbf{v}^\pi$ for the variable \mathbf{v}_ϕ^π . In all our experiments we always found that the left Moore-Penrose pseudo-inverse of Φ exists, because the rows of the matrix Φ span all n dimensions, where n is the dimension of the learned feature representation. The following sections will present empirical results on two example MDPs and discuss why the row space of Φ spans all n dimensions.

Algorithm 2 Feature Policy Evaluation

- 1: Given \mathbf{P}_ϕ^a , \mathbf{r}_ϕ^a , and policy matrices $\Pi^a \forall a$.
 - 2: **repeat**
 - 3: $\mathbf{q}_\phi^a \leftarrow \mathbf{r}_\phi^a + \gamma \mathbf{P}_\phi^a \mathbf{v}_\phi^\pi \forall a \in \mathcal{A}$
 - 4: $\mathbf{v}_\phi^\pi \leftarrow \Phi^+ \sum_a \Pi^a \Phi \mathbf{q}_\phi^a$ { Φ^+ is the pseudo-inverse}
 - 5: **until** \mathbf{v}_ϕ^π converges
-

4.4.1 COLUMN GRID WORLD

We tested our implementation on the column world shown in Figure 1. In column world transitions are deterministic and the gradient is computed for each transition individually. Because the feature representation is linear in a one-hot state representation (Eq. (53)), the feature matrix Φ is obtained by minimizing the loss objective

$$\sum_{a \in \mathcal{A}} \|\Phi \mathbf{r}_\phi^a - \mathbf{r}^a\|_2 + \alpha \frac{1}{|\mathcal{S}|} \|\Phi + \gamma \mathbf{P}^a \Phi \mathbf{F}^\pi - \Phi \mathbf{F}^a\|_2. \quad (55)$$

The factor $\frac{1}{|\mathcal{S}|}$ appears in Eq. (55) because the L2 matrix norm sums the L2 norm of each row rather than averaging over all rows. Optimizing the loss objective in Eq. (55) with a gradient optimizer is equivalent to performing batch gradient descent on the loss objective in Eq. (52).

Figure 1(c) shows the initial feature representation which was sampled uniformly at random. Figures 1(d), 1(e), and 1(f) show how the feature representation evolves as the loss objective is optimized. One can observe that after 1000 gradient steps, the learned feature representation assigns approximately the same feature vector to bisimilar states.

In that sense the learned feature representation is an approximation of a model reduction. Figure 3 plots the value error for a range of ε -greedy policies at each gradient iteration. Each ε -greedy policy selects actions uniformly at random with ε probability and otherwise selects the optimal action. Because the discount factor was set to $\gamma = 0.9$, the value function can span the interval $[0, 10]$. One can observe that after around 400 iterations the value error of each tested policy is comparably small. During training, uniform random action selection ($\varepsilon = 1$) has the lowest prediction error and prediction errors increase as ε tends to zero and the policy becomes more similar to the optimal policy. This behaviour is expected because the SF representation was trained for uniform random action selection and approximation errors limit the learned representation’s ability to generalize to different policies. In this experiment we found that Assumption 1 may not hold during training, however, the value error was comparably small and Algorithm 1 always converged to a solution. Appendix B lists all hyper parameters needed to reproduce this experiment.

Because we use a linear action model, feature-to-feature transitions are modelled with a matrix multiplication. If the feature representation ϕ maps states to one-hot bit vectors, then any particular transition function can be represented with stochastic transition matrices $\{\mathbf{P}_\phi^a\}_a$. Hence if the learned cluster centers in Figure 1(f) would all fall on some one-hot bit vector, then this solution would have a zero loss value. Because the solution learned for column world is approximate, the feature centers in Figure 1(f) only form a linearly independent set and the learned feature vectors do not fall exactly on the cluster centers. However, the number of bisimilar partitions still appears in the form of the feature dimensions of the learned solution, because in three dimensions one can only represent at most three linearly independent vectors. Because the feature representation approximately clustered into 3 linearly independent vectors and because it is initialized uniformly at random, the feature matrix Φ has a row-space spanning all three dimensions. A similar argument applies to the following puddle world experiments.

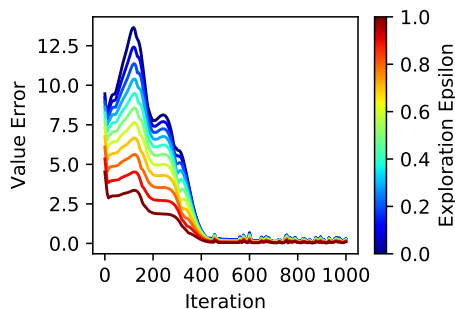


Figure 3: Column world value error for different ε -greedy policies.

4.4.2 PUDDLE WORLD EXPERIMENTS

Puddle world (Boyan and Moore, 1995) is a grid-world navigation task where the agent has to navigate to a goal location to collect a +1 reward while avoiding a puddle. Figure 4(a) shows a map of puddle world. Entering a puddle grid cell results in -0.5 reward for each transition. The agent selects one out of four actions to move up, down, left, or right. Transitions are successful with 90% probability and with a 10% probability will result in a transition to a cell orthogonal to the intended direction or the agent does not move.

The only perfect model reduction on the state space of puddle world is the identity map. Suppose two adjacent states are clustered. Then, the compressed state space would lose

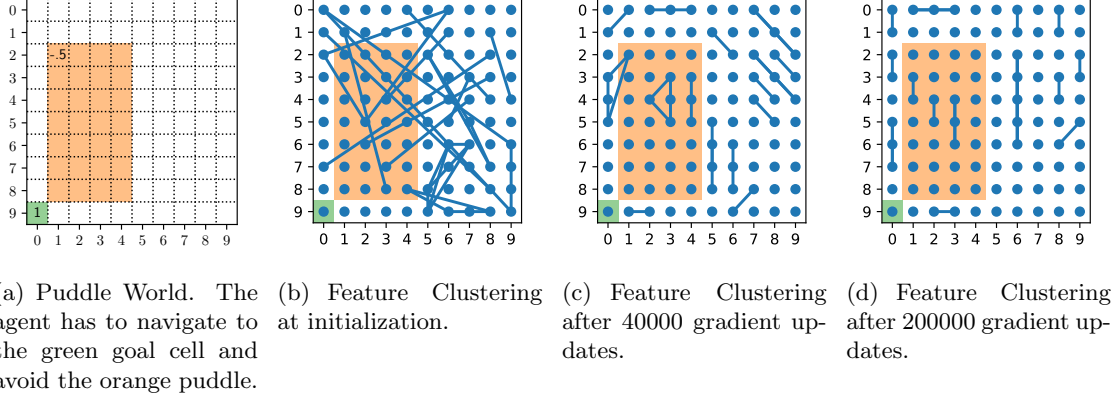


Figure 4: Puddle world map and the learned partitioning of the state space.

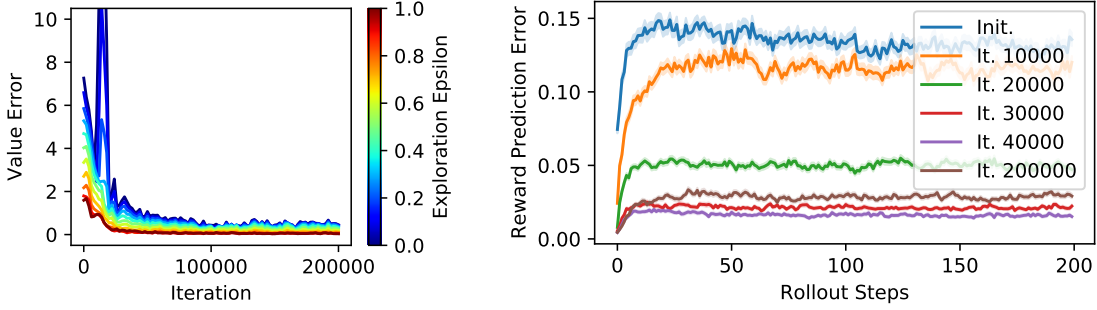


Figure 5: Puddle World Prediction Errors.

the exact position information in the grid, rendering accurate predictions about expected future rewards impossible if only the compressed feature model is used.

Stochastic gradient descent was used to learn a feature representation for puddle world. To further stabilize training, the SF target was assumed to be fixed and no gradients are computed through it. Given a transition data set, the following expectation was sampled:

$$\mathbb{E} \left[\left(\phi_s^\top \mathbf{r}_\phi^a - r(s, a) \right)^2 + \alpha \left\| \phi_s^\top \mathbf{F}^a - \mathbf{y}_{s,a,r,s'} \right\|_2^2 \right], \quad (56)$$

where $\mathbf{y}_{s,a,r,s'} = \phi_s^\top + \gamma \phi_{s'}^\top \mathbf{F}^\pi$ is the SF target (similar to the SF-learning algorithm). The transition data set for puddle world was generated by iterating over the state space and sampling one transition starting at each state, until the transition data set of 1000 transitions is reached. Actions were sampled uniformly at random to generate a transition.

To access which representations approximate model features find, we constrained the feature representation to 80 dimensions, effectively forcing the algorithm to over-compress

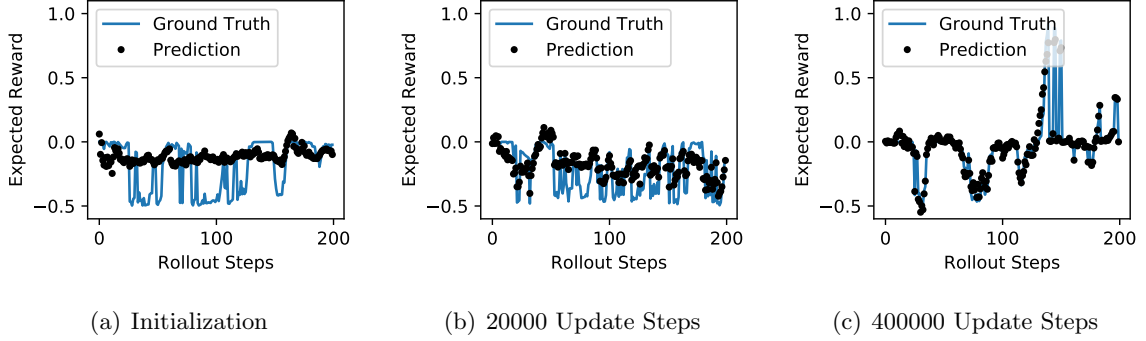


Figure 6: Example rollouts on puddle world.

the state space into 80 linearly independent features and to introduce some approximation error. During different stages of training, the feature vector for each state was computed and this set of vectors was clustered into 80 clusters using k-Means clustering (Bishop, 2006). Figures 4(b), 4(c), and 4(d) illustrate the found clustering by linking states together that have the same closest cluster centroid in common. Figure 4(b) shows the clustering obtained for the feature initialization, where feature vectors are sampled uniformly at random. One can observe that through training (Figures 4(c) and 4(d)) clusters that contain states that are far apart in the grid are broken up and states that are close together in the grid are mapped to feature vectors that are close together in terms of their euclidean L2 norm. As expected, the approximate feature representation attempts to preserve the position in the grid in order to ensure accurate predictions of future reward sequences and thus resembles an approximate model reduction.

Overall, stochastic gradient descent was performed on the loss objective \mathcal{L} for 200000 steps. Figure 5 shows the prediction errors for the learned feature representation at different stages of training. Initially value errors are high but are reduced significantly during training (Figure 5(a)). Similar to the column world experiments, uniform random action selection ($\varepsilon = 1$) produces the lowest value errors, because the SFs are trained for this policy. As ε is decreased and the policy becomes more similar to the (greedy) optimal policy, value errors increase because to some extent approximation errors limit the learned representation to generalize to arbitrarily different policies. However, at the end of training all policies can be predicted with comparably low value errors. Note that Figure 5(a) plots for each policy the highest absolute value difference $\left\| \Phi \mathbf{v}_\phi^\pi - \mathbf{v}^\pi \right\|_\infty$ (the maximum is computed over all 100 states). Figure 5(b) plots the expected reward prediction error for 200 step action sequences. For each curve, 100 state and action sequence pairs (s, a_1, \dots, a_{200}) were sampled uniformly at random and the expected reward was computed for each time step using the feature model. The expected reward errors fall into the interval $[0, 1.5]$. At initialization, expected reward prediction errors are at a comparably high level and then decrease to about 0.025 as training progresses. Because model features directly attempt to approximate a model reduction and effectively learn a multi-step model, the reward prediction error curves move horizontally down as training progresses. The discount factor γ discounts the n step feature prediction errors with γ^n . Increasing the discount factor γ towards one then results in

the model assigning more weight to predictions that range over longer time steps. In this experiment, the discount factor $\gamma = 0.9$ and thus choosing a 200 step rollout length is sufficient to estimate a γ -discounted value function: if rewards that lie 200 time steps into the future were predicted uniformly at random in the interval $[-0.5, 1]$, then the value error can be influenced by at most $0.9^{200} \cdot 1.5 \approx 1.1 \cdot 10^{-9}$. If the goal is to predict rewards further than 200 time steps into the future, then one would have to further increase the discount factor γ .

Figure 6 shows three example rollouts at three different stages during training. We only evaluate expected future rewards. Because the transition function is stochastic, the reward prediction curves in Figure 6 are averaged over multiple reward values and are thus smoothed. All hyper-parameters for the puddle world experiment are documented in Appendix B.

5. Discussion

We demonstrate how SFs can be used for model-based RL by learning a feature representation and optimizing over the space of all possible value functions. Given a fixed basis function, Section 3 shows how learning SFs is equivalent to learning value functions through Q-learning. However, Q-learning does not only evaluate a particular control policy but also searches for the optimal policy. For finite state and action spaces, Strehl et al. (2006) show that such model-free algorithms have a sample complexity exponential in the size of the state space and converge much slower than model-based algorithms such as RMax (Strehl et al., 2009). A similar argument applies for learning SFs. For finite state and action spaces and given a fixed policy $\bar{\pi}$, the SFs for this policy can be directly computed with $\mathbf{F}^a = \mathbf{I} + \gamma \mathbf{P}^a \mathbf{F}^{\bar{\pi}}$ and $\mathbf{F}^{\bar{\pi}} = (\mathbf{I} - \gamma \mathbf{P}^{\bar{\pi}})^{-1}$, which are both at most $O(|\mathcal{S}|^3 |\mathcal{A}|)$ operations⁴. Section 3 shows how this complexity of estimating SFs changes when SFs are also used to search for the optimal policy and that learning SFs effectively resembles model-free learning. Consequently, given any particular feature representation ϕ , feature-reward model $\{\mathbf{r}_\phi^a\}_a$, and feature-to-feature transition matrices $\{\mathbf{P}_\phi^a\}_a$, the SFs can be computed for this model in polynomial time. However, the computational complexity of computing model reductions or approximations thereof still remains an open problem. Existing literature shows that under different assumptions, computing state abstractions that compress the state space maximally is NP-hard (Even-Dar and Mansour, 2003; Abel et al., 2018).

One open question central to model-based RL is how to handle approximation errors. Existing theoretical results assume that single step transition models are approximated directly. If an approximate single-step model is used for rollout predictions, approximation errors compound resulting in poor accuracy. Because of this compounding effect, existing prediction error bounds have an exponential dependency on the rollout length T (Talvitie, 2017; Asadi et al., 2018). SFs predict the visitation frequencies over future state visitations and thus intuitively encode a discounted infinite-step model. This property allows SFs to be tied to bisimulations, which define an equivalence criterion recursively on the transition function. The approximation bounds presented in Section 4.3 show how the discount factor γ influences the accuracy of the learned model. Specifically, the accuracy of predicting the visitation frequency 100 time steps into the future is discounted with a factor of γ^{100} .

4. In this case the matrix \mathbf{F}^a is an action conditioned version of the SR matrix $\Psi_{\text{SR}}^{\bar{\pi}}$.

Hence approximation errors still compound and reward predictions that lie T time steps into the future will generally increase as T increases. In contrast to existing work our bounds scale linearly in the approximation errors ε_ψ and ε_r . Further, the discount factor provides a variable to control how far into the future the approximate model should be able to provide accurate predictions. Lehnert et al. (2018) show how finding an ε -approximation of a discounted value function becomes increasingly difficult if the discount factor tends to one and the planning horizon increases. One would expect a similar result for SFs, because as γ tends to one the learned model is required to provide accurate predictions over an increasingly long planning horizon.

Consequently, this result raises the question how much transition experience is needed to accurately approximate SFs versus approximating a single-step transition model. Future work would explore the design of efficient learning algorithms and compare learning SFs to single-step transition models. The presented gradient-based approximation method may also open the door to using neural networks and deep learning techniques to learn model reductions. Existing model-based deep RL methods either augment a model-free learning algorithm, similar to DQN (Mnih et al., 2015), with model-based techniques to accelerate learning (Oh et al., 2017; Weber et al., 2017), or learn an auto-encoder structure on the state space and demonstrate good performance on certain benchmarks (Finn et al., 2015; Ha and Schmidhuber, 2018). One fundamental shortcoming of an auto-encoder based approach is that the feature representation is targeted towards reconstructing the state and not predicting future reward outcomes. Finn et al. (2015) or Ha and Schmidhuber (2018) are only able to demonstrate good performance on domains where the state is represented as an image and the most visually salient features coincide with the features that are important for constructing reward predictions. However, how to solve any game of the Atari 2600 benchmark (Bellemare et al., 2012) using a “strict” model-based algorithm still remains an open problem. While there exist different algorithms to learn SFs with a deep neural network (Kulkarni et al., 2016; Barreto et al., 2018; Zhang et al., 2016), these methods do not implement the linear action model we present in this paper. How to design deep learning algorithms to learn model reductions is left to future work and beyond the scope of this paper.

The presented model is similar to Linear Dyna (Sutton et al., 2008) and LAMs (Yao and Szepesvári, 2012); the key advantage of using model features is that they are learned with the purpose of providing accurate rollout predictions. In RL, hard-coding a feature representation has been common practice in the form of defining basis functions (Sutton, 1996; Konidaris et al., 2011; Parr et al., 2008) and for linear value function approximation algorithms such as LSTD (Boyan, 1999) were developed. While Algorithm 2 does not perform LSTD, LSTD can be used with model features without any modifications. If $\varepsilon_r = 0$ and $\varepsilon_\psi = 0$, then any value function can be expressed linearly with model features without any approximation errors. In this case, LSTD does not provide any benefits over TD-learning (Sutton, 1988).

Talvitie (2018) presents a model of learning to predict rewards for approximate transition models. Because approximate transition models produce an approximation of a future state, this approximation need not resemble an actual state (Talvitie, 2017). As a result, a reward predictor trained to predict rewards given an actual state cannot be directly used. Model features address this problem because a feature space is constructed in which predictions

are linear. The presented theoretical results show how the learned reward model $\{\mathbf{r}_\phi^a\}_a$ can be used for multi-step predictions without tying training to the approximate transition model.

Song et al. (2016) present a framework for simultaneously encoding the transition and reward functions of an MDP. However, one key distinction from model features is that Song et al.’s model uses an encoder and decoder to find a feature representation. Model features do not need a decoding step and thus compress the state space into a smaller representation. Similar to the work of Parr et al. (2008), model features also find a linear approximation of the transition and reward functions. Model features extract a linear single-step transition function from the learned successor features. Importantly, because model features approximate model reductions, the feature space encodes the transition and reward function linearly without any approximation error, if $\varepsilon_r = 0$ and $\varepsilon_\psi = 0$. This property distinguishes model features from any previous analysis of Linear Action Models: As approximation errors vanish in the limit during training, any representation and prediction errors vanish as well.

Our method is the first direct gradient optimization approach to learning approximate model reductions. Recently, Ruan et al. (2015) presented algorithms to cluster approximately bisimilar states. Their method relies on bisimulation metrics (Ferns et al., 2004), which use the Wasserstein metric to assess if two state transitions have the same distribution over next state clusters. In contrast to their approach, we phrase learning a model reduction as learning a feature representation, which ultimately leads to an energy minimization problem and our theoretical analysis also applies to continuous state spaces. The presented error bounds can be used to access prediction errors if the state space is compressed into too few clusters.

Russek et al. (2017) and Momennejad et al. (2017) show that SFs incorporate elements from model-free and model-based RL and that SFs can be used to explain transfer learning in humans. Existing work, for example Dayan (1993); Barreto et al. (2018); Lehnert et al. (2017), view SFs as a method for encoding visitation frequencies of a particular policy, allowing the policy to be immediately evaluated against different reward functions, because SFs are obtained by extracting the reward model from value functions. In that sense, SFs have been understood as an intermediate representation between model-free and model-based RL algorithms, because the reward function is stored separately (as in Algorithm 1) from SFs which resemble a value function like structure. This paper presents a different perspective on model-free and model-based RL uncovering a novel connection between SFs and model-based RL. Ultimately, model features do not depend on a specific policy like SFs do and model features can be thought of as a knowledge representation, because they encode which parts of the agent’s environment are important to distinguish.

6. Conclusion

This presented results highlight how learning successor features is equivalent to Q-learning, but when successor features are used for representation learning one obtains an approximation of model features, which encode model reductions. Model reductions can be understood as a knowledge representation of a given control task, because they encode which states are behaviourally equivalent and which should be treated as distinct. Model features provide

a novel perspective on model-based RL: Rather than learning a single step transition predictor, they learn a feature representation tailored to predict multi-step rollouts. The key advantage of this approach is how approximation errors are handled. By only approximating a single step transition model, prediction errors compound quickly when computing the expected future reward using this approximate model. Instead, model features are learned by approximating SFs, which encode multi-step models. Hence, if a feature representation is rich enough to predict accurate SFs and one-step rewards, then it is also rich enough to accurately predict future reward outcomes. We hope that model features can be used to guide the design of novel approximate model-based RL algorithms.

Appendix A. Proofs of Theoretical Results

Theorem 1 states under which assumptions SF-learning and linear Q-learning are equivalent. The proof is by induction on the number of iterations SF-learning and linear Q-learning are executed.

Proof of Theorem 1. The proof is by induction on t .

Base Case: For $t = 1$,

$$\mathbf{w}^\top \mathbf{F}_1 = \mathbf{w}^\top \left(\mathbf{F}_0 + \alpha_\psi \left(\phi_{s,a} + \gamma \mathbf{F}_0 \phi_{s',a^*} - \mathbf{F}_0 \phi_{s,a} \right)^\top \phi_{s,a} \right) \quad (57)$$

$$= \mathbf{w}^\top \mathbf{F}_0 + \alpha_\psi \left(\mathbf{w}^\top \phi_{s,a} + \gamma \mathbf{w}^\top \mathbf{F}_0 \phi_{s',a^*} - \mathbf{w}^\top \mathbf{F}_0 \phi_{s,a} \right)^\top \phi_{s,a} \quad (58)$$

$$= \boldsymbol{\theta}_0^\top + \alpha_\psi \left(\mathbf{w}^\top \phi_{s,a} + \gamma \mathbf{w}^\top \mathbf{F}_0 \phi_{s',a^*} - \mathbf{w}^\top \mathbf{F}_0 \phi_{s,a} \right)^\top \phi_{s,a} \quad (59)$$

$$= \boldsymbol{\theta}_0^\top + \alpha_\psi \left(r(s, a) + \gamma \boldsymbol{\theta}_0^\top \phi_{s',a^*} - \boldsymbol{\theta}_0^\top \phi_{s,a} \right)^\top \phi_{s,a} \quad (60)$$

$$= \boldsymbol{\theta}_1^\top. \quad (61)$$

Because actions are selected using a control policy $\eta : s, Q(s, \cdot), t \mapsto a$, the action selected at the next time step is the same for both algorithms.

Induction Step: Assume $\mathbf{w}^\top \mathbf{F}_t = \boldsymbol{\theta}_t^\top$ holds for t , then

$$\mathbf{w}^\top \mathbf{F}_{t+1} = \mathbf{w}^\top \left(\mathbf{F}_t + \alpha_\psi \left(\phi_{s,a} + \gamma \mathbf{F}_t \phi_{s',a^*} - \mathbf{F}_t \phi_{s,a} \right)^\top \phi_{s,a} \right) \quad (62)$$

$$= \mathbf{w}^\top \mathbf{F}_t + \alpha_\psi \left(\mathbf{w}^\top \phi_{s,a} + \gamma \mathbf{w}^\top \mathbf{F}_t \phi_{s',a^*} - \mathbf{w}^\top \mathbf{F}_t \phi_{s,a} \right)^\top \phi_{s,a} \quad (63)$$

$$= \boldsymbol{\theta}_t^\top + \alpha_\psi \left(\mathbf{w}^\top \phi_{s,a} + \gamma \mathbf{w}^\top \mathbf{F}_t \phi_{s',a^*} - \mathbf{w}^\top \mathbf{F}_t \phi_{s,a} \right)^\top \phi_{s,a} \quad (64)$$

$$= \boldsymbol{\theta}_t^\top + \alpha_\psi \left(r(s, a) + \gamma \boldsymbol{\theta}_t^\top \phi_{s',a^*} - \boldsymbol{\theta}_t^\top \phi_{s,a} \right)^\top \phi_{s,a} \quad (65)$$

$$= \boldsymbol{\theta}_{t+1}^\top. \quad (66)$$

Because actions are selected using a control policy $\eta : s, Q(s, \cdot), t \mapsto a$, the action selected at the next time step is the same for both algorithms. \square

Lemma 1 states that given a matrix \mathbf{F}^a that satisfies the SF fix-point Eq. (37), then there exists left-stochastic partition-to-partition transition matrices $\{\mathbf{P}_{\phi,\omega}^a\}_a$ for every weighting

function ω . Intuitively, the weighting function specifies the probability with which a state is encountered in a partition and can also be understood as specifying visitation frequencies over the state space. These visitation frequencies effect the observed partition-to-partition transition probabilities. The proof of Lemma 1 uses this intuition.

Proof of Lemma 1. Let $\overset{\phi}{\sim}$ be an equivalence relation induced by the feature representation ϕ such that for any pair of states s and s' ,

$$s \overset{\phi}{\sim} s' \iff \phi_s = \phi_{s'}. \quad (67)$$

We denote elements of the quotient set induced by $\overset{\phi}{\sim}$ as $\mathcal{B}(\phi_s) \in \mathcal{S}/\overset{\phi}{\sim}$, where $\mathcal{B}(\phi_s)$ is the partition of states that map to the same one-hot bit vector ϕ_s the state s maps to.

For a discrete state spaces \mathcal{S} , pick an arbitrary weighting function ω and an arbitrary $\mathcal{B}(\phi_s) \in \mathcal{S}/\overset{\phi}{\sim}$. Then, the probability of transitioning from ϕ_s to $\phi_{s'}$ can be written as

$$\Pr_{\omega}\{\phi_s \xrightarrow{a} \phi_{s'}\} = \sum_{s \in \mathcal{B}(\phi_s)} \omega(s) \Pr\{s \xrightarrow{a} \phi_{s'}\} \quad (68)$$

For a continuous state space \mathcal{S} , pick an arbitrary weighting function ω and an arbitrary $\mathcal{B}(\phi_s) \in \mathcal{S}/\overset{\phi}{\sim}$. Then, the probability of transitioning from ϕ_s to $\phi_{s'}$ can be written as

$$\Pr_{\omega}\{\phi_s \xrightarrow{a} \phi_{s'}\} = \int_{s \in \mathcal{B}(\phi_s)} \omega(s) \Pr\{s \xrightarrow{a} \phi_{s'}\} ds \quad (69)$$

For both cases a stochastic feature-to-feature transition matrix $\mathbf{P}_{\phi, \omega}^a$ can be constructed by setting each entry to

$$\mathbf{P}_{\phi, \omega}^a(i, j) = \Pr_{\omega}\{\mathbf{e}_j \xrightarrow{a} \mathbf{e}_i\}. \quad (70)$$

For the discrete case we have

$$\sum_{s \in \mathcal{B}(\phi_s)} \omega(s) \phi_s^{\top} \mathbf{F}^a = \left(\sum_{s \in \mathcal{B}(\phi_s)} \omega(s) \right) \phi_s^{\top} \mathbf{F}^a = \phi_s^{\top} \mathbf{F}^a, \quad (71)$$

where the second step follows from the fact that $\phi_s = \phi_{\tilde{s}}$ for $s, \tilde{s} \in \mathcal{B}(\phi_s)$. Hence

$$\phi_s^{\top} \mathbf{F}^a = \sum_{s \in \mathcal{B}(\phi_s)} \omega(s) \left(\phi_s^{\top} + \gamma \mathbb{E} \left[\phi_{s'}^{\top} \mathbf{F}^{\bar{\pi}} \middle| s, a \right] \right) \quad (72)$$

$$= \phi_s^{\top} + \gamma \left(\sum_{s \in \mathcal{B}(\phi_s)} \omega(s) \mathbb{E} \left[\phi_{s'}^{\top} \middle| s, a \right] \right) \mathbf{F}^{\bar{\pi}} \quad (73)$$

$$= \phi_s^{\top} + \gamma \left(\sum_{s \in \mathcal{B}(\phi_s)} \omega(s) \sum_{i=1}^n \Pr\{s \xrightarrow{a} \mathbf{e}_i\} \mathbf{e}_i^{\top} \right) \mathbf{F}^{\bar{\pi}} \quad (74)$$

$$= \phi_s^{\top} + \gamma \left(\sum_{i=1}^n \sum_{s \in \mathcal{B}(\phi_s)} \omega(s) \Pr\{s \xrightarrow{a} \mathbf{e}_i\} \mathbf{e}_i^{\top} \right) \mathbf{F}^{\bar{\pi}} \quad (75)$$

$$= \phi_s^{\top} + \gamma \phi_s^{\top} \mathbf{P}_{\phi, \omega}^a \mathbf{F}^{\bar{\pi}} \quad (76)$$

The continuous case can be proven similarly. Assuming an arbitrary weighting function ω and partition $\mathcal{B}(\phi_s)$,

$$\int_{s \in \mathcal{B}(\phi_s)} \omega(s) \phi_s^\top \mathbf{F}^a ds = \left(\int_{s \in \mathcal{B}(\phi_s)} \omega(s) ds \right) \phi_s^\top \mathbf{F}^a = \phi_s^\top \mathbf{F}^a, \quad (77)$$

and

$$\phi_s^\top \mathbf{F}^a = \int_{s \in \mathcal{B}(\phi_s)} \omega(s) \left(\phi_s^\top + \gamma \mathbb{E} \left[\phi_{s'}^\top \mathbf{F}^{\bar{\pi}} \middle| s, a \right] \right) ds \quad (78)$$

$$= \phi_s^\top + \gamma \left(\int_{s \in \mathcal{B}(\phi_s)} \omega(s) \mathbb{E} \left[\phi_{s'}^\top \mathbf{F}^{\bar{\pi}} \middle| s, a \right] ds \right) \mathbf{F}^{\bar{\pi}} \quad (79)$$

$$= \phi_s^\top + \gamma \left(\int_{s \in \mathcal{B}(\phi_s)} \omega(s) \sum_{i=1}^n \Pr\{s \xrightarrow{a} \mathbf{e}_i\} \mathbf{e}_i^\top ds \right) \mathbf{F}^{\bar{\pi}} \quad (80)$$

$$= \phi_s^\top + \gamma \sum_{i=1}^n \left(\int_{s \in \mathcal{B}(\phi_s)} \omega(s) \Pr\{s \xrightarrow{a} \mathbf{e}_i\} ds \right) \mathbf{e}_i^\top \mathbf{F}^{\bar{\pi}} \quad (81)$$

$$= \phi_s^\top + \gamma \sum_{i=1}^n \Pr\{\phi_s \xrightarrow{a} \mathbf{e}_i\} \mathbf{e}_i^\top \mathbf{F}^{\bar{\pi}} \quad (82)$$

$$= \phi_s^\top + \gamma \phi_s^\top \mathbf{P}_{\phi, \omega}^a \mathbf{F}^{\bar{\pi}}. \quad (83)$$

For both discrete and continuous state spaces the identity $\phi_s^\top \mathbf{F}^a = \phi_s^\top + \gamma \phi_s^\top \mathbf{P}_{\phi, \omega}^a \mathbf{F}^{\bar{\pi}}$ holds for every $\phi_s = \mathbf{e}_i$ for some i . Because ω and the action a were assumed to be arbitrary, we have that

$$\forall \omega, \exists \{\mathbf{P}_{\phi, \omega}^a\}_a : \mathbf{F}^a = \mathbf{I} + \gamma \mathbf{P}_{\phi, \omega}^a \mathbf{F}^{\bar{\pi}}. \quad (84)$$

From Eq. (84) we can prove both statements: The inverse of the matrix $\mathbf{F}^{\bar{\pi}}$ exists because $\mathbf{P}_{\phi, \omega}^a$ is a stochastic matrix and

$$\mathbf{F}^{\bar{\pi}} = \mathbf{I} + \gamma \mathbf{P}_{\phi, \omega}^{\bar{\pi}} \mathbf{F}^{\bar{\pi}} \iff \mathbf{F}^{\bar{\pi}} = (\mathbf{I} - \gamma \mathbf{P}_{\phi, \omega}^{\bar{\pi}})^{-1}. \quad (85)$$

Using the inverse of $\mathbf{F}^{\bar{\pi}}$ we can re-write Eq. (84) and obtain

$$\mathbf{P}_{\phi, \omega}^a = \frac{1}{\gamma} (\mathbf{F}^a - \mathbf{I}) (\mathbf{F}^{\bar{\pi}})^{-1}. \quad (86)$$

Eq. (86) shows that $\mathbf{P}_{\phi, \omega}^a$ does not depend on ω and that we have

$$\forall \omega, \omega', \mathbf{P}_{\phi, \omega}^a = \mathbf{P}_{\phi, \omega'}^a = \mathbf{P}_{\phi}^a, \quad (87)$$

as desired. \square

Using Lemma 1, we can show that SFs encode model reductions and prove Theorem 2.

Proof of Theorem 2. To show that ϕ is a model-feature, we have to show that for any state pair s and \tilde{s} ,

$$\phi_s = \phi_{\tilde{s}} \implies s \stackrel{b}{\sim} \tilde{s}. \quad (88)$$

Suppose $\phi_s = \phi_{\tilde{s}}$ holds, then $r(s, a) = \phi_s^\top \mathbf{r}_\phi^a = \phi_{\tilde{s}}^\top \mathbf{r}_\phi^a = r(\tilde{s}, a)$ and the reward condition in Definition 2 holds. Using the fact that both s and \tilde{s} are mapped to the same SFs, we obtain

$$\phi_s^\top \mathbf{F}^a = \phi_{\tilde{s}}^\top \mathbf{F}^a \quad (89)$$

$$\phi_s^\top + \gamma \mathbb{E} \left[\phi_{s'}^\top \mathbf{F}^\pi \middle| s, a \right] = \phi_{\tilde{s}}^\top + \gamma \mathbb{E} \left[\phi_{\tilde{s}'}^\top \mathbf{F}^\pi \middle| \tilde{s}, a \right] \quad (90)$$

$$\mathbb{E} \left[\phi_{s'}^\top \mathbf{F}^\pi \middle| s, a \right] = \mathbb{E} \left[\phi_{\tilde{s}'}^\top \mathbf{F}^\pi \middle| \tilde{s}, a \right] \quad (91)$$

$$\mathbb{E} \left[\phi_{s'}^\top \middle| s, a \right] = \mathbb{E} \left[\phi_{\tilde{s}'}^\top \middle| \tilde{s}, a \right] \quad (\text{because } (\mathbf{F}^\pi)^{-1} \text{ exists by Lemma 1}) \quad (92)$$

$$\sum_{i=1}^n \Pr \left\{ s \xrightarrow{a} \mathbf{e}_i \right\} \mathbf{e}_i = \sum_{i=1}^n \Pr \left\{ \tilde{s} \xrightarrow{a} \mathbf{e}_i \right\} \mathbf{e}_i. \quad (93)$$

Because \mathbf{e}_i is a one-hot bit vector, an expectation over a finite set of one-hot bit vectors contains the corresponding probability values in each entry of the vector. Hence $\Pr \left\{ s \xrightarrow{a} \mathbf{e}_i \right\} = \Pr \left\{ \tilde{s} \xrightarrow{a} \mathbf{e}_i \right\}$ for all i , and thus the transition model condition in Definition 2 holds. To see why the inverse of the matrix \mathbf{F}^π exists, refer to the end of the proof of Lemma 1. \square

The following lemma relates the SF approximation error ε_ψ to the one-step feature model prediction error.

Lemma 2 (Transition Model Error). *Consider an MDP $M = \langle \mathcal{S}, \mathcal{A}, p, r, \gamma \rangle$ and assume that ε_r and ε_ψ are defined as in Eq. (47) and Eq. (48), then*

$$\gamma \left\| \phi_s^\top \mathbf{P}_\phi^a - \mathbb{E}_{s'} \left[\phi_{s'}^\top \middle| s, a \right] \right\|_2 \leq \varepsilon_\psi (1 + \gamma). \quad (94)$$

Proof. By Assumption 1, we note that \mathbf{F}^π has an inverse, because $\mathbf{F}^\pi = (\mathbf{I} - \gamma \mathbf{P}_\phi^\pi)^{-1}$. The norm of $(\mathbf{F}^\pi)^{-1}$ can be bounded with

$$\left\| (\mathbf{F}^\pi)^{-1} \right\|_2 = \left\| \mathbf{I} - \gamma \mathbf{P}_\phi^\pi \right\|_2 \leq 1 + \gamma \left\| \mathbf{P}_\phi^\pi \right\|_2 \leq 1 + \gamma.$$

Hence we can write

$$\phi_s^\top + \gamma \mathbb{E}_{s'} \left[\phi_{s'}^\top \mathbf{F}^\pi \middle| s, a \right] - \phi_s^\top \mathbf{F}^a = \phi_s^\top + \gamma \mathbb{E}_{s'} \left[\phi_{s'}^\top \mathbf{F}^\pi \middle| s, a \right] - \phi_s^\top (\mathbf{I} + \gamma \mathbf{P}_\phi^a \mathbf{F}^\pi) \quad (95)$$

$$= \gamma \left(\mathbb{E}_{s'} \left[\phi_{s'}^\top \middle| s, a \right] + \phi_s^\top \mathbf{P}_\phi^a \right) \mathbf{F}^\pi \quad (96)$$

Bounding the L2 norm gives

$$\gamma \left\| \left(\mathbb{E}_{s'} \left[\phi_{s'}^\top |s, a\right] + \phi_s^\top \mathbf{P}_\phi^a \right) \mathbf{F}^\pi (\mathbf{F}^\pi)^{-1} \right\|_2 \quad (97)$$

$$= \left\| \gamma \left(\mathbb{E}_{s'} \left[\phi_{s'}^\top |s, a\right] + \phi_s^\top \mathbf{P}_\phi^a \right) \right\|_2 \quad (98)$$

$$= \left\| \left(\phi_s^\top + \gamma \mathbb{E}_{s'} \left[\phi_{s'}^\top \mathbf{F}^\pi |s, a\right] - \phi_s^\top \mathbf{F}^a \right) (\mathbf{F}^\pi)^{-1} \right\|_2 \quad (99)$$

$$\leq \left\| \phi_s^\top + \gamma \mathbb{E}_{s'} \left[\phi_{s'}^\top \mathbf{F}^\pi |s, a\right] - \phi_s^\top \mathbf{F}^a \right\|_2 \left\| (\mathbf{F}^\pi)^{-1} \right\|_2 \quad (100)$$

$$\leq \varepsilon_\psi (1 + \gamma). \quad (101)$$

□

Using Lemma 2 we can proof both approximation bound theorems.

Proof of Theorem 3. The proof is by induction on T .

Base Case: For $T = 1$,

$$\left| \phi_s^\top \mathbf{r}_\phi^{a_1} - \mathbb{E}_{s'} \left[\phi_{s'}^\top \mathbf{r}_\phi^{a_1} |s, a_1\right] \right| \leq \varepsilon_r. \quad (102)$$

Induction Step: Assume that the bound holds for T , then for $T + 1$,

$$\left| \phi_s^\top \mathbf{P}_\phi^{a_1} \dots \mathbf{P}_\phi^{a_T} \mathbf{r}_\phi^{a_{T+1}} - \mathbb{E}_{s'} \left[\phi_{s'}^\top \mathbf{r}_\phi^{a_{T+1}} |s, a_1, \dots, a_{T+1}\right] \right| \quad (103)$$

$$\leq \left| \phi_s^\top \mathbf{P}_\phi^{a_1} \dots \mathbf{P}_\phi^{a_T} \mathbf{r}_\phi^{a_{T+1}} - \mathbb{E}_{s_2} \left[\phi_{s_2}^\top \mathbf{P}_\phi^{a_2} \dots \mathbf{P}_\phi^{a_T} \mathbf{r}_\phi^{a_{T+1}} |s, a_1\right] \right| \quad (104)$$

$$+ \left| \mathbb{E}_{s_2} \left[\phi_{s_2}^\top \dots \mathbf{P}_\phi^{a_T} \mathbf{r}_\phi^{a_{T+1}} |s, a_1\right] - \mathbb{E}_{s'} \left[\phi_{s'}^\top \mathbf{r}_\phi^{a_{T+1}} |s, a_1, \dots, a_{T+1}\right] \right| \quad (105)$$

$$\leq \left\| \phi_s^\top \mathbf{P}_\phi^{a_1} - \mathbb{E}_{s'} \left[\phi_{s'}^\top |s, a_1\right] \right\|_2 \left\| \mathbf{P}_\phi^{a_2} \dots \mathbf{P}_\phi^{a_T} \mathbf{r}_\phi^{a_{T+1}} \right\|_2 \quad (106)$$

$$+ \left| \mathbb{E}_{s_2} \left[\phi_{s_2}^\top \dots \mathbf{P}_\phi^{a_T} \mathbf{r}_\phi^{a_{T+1}} - \mathbb{E}_{s'} \left[\phi_{s'}^\top \mathbf{r}_\phi^{a_{T+1}} |s_2, a_2, \dots, a_{T+1}\right] \right] |s, a_1\right| \quad (107)$$

$$\leq \frac{\varepsilon_\psi (1 + \gamma)}{\gamma} \max_a \left\| \mathbf{r}_\phi^a \right\|_2 + \varepsilon_r + \frac{(T - 1)(1 - \gamma)}{\gamma} \varepsilon_\psi \left\| \mathbf{r}_\phi^{a_T} \right\|_2 \quad (108)$$

$$= \varepsilon_r + \frac{T(1 - \gamma)}{\gamma} \varepsilon_\psi \max_a \left\| \mathbf{r}_\phi^a \right\|_2 \quad (109)$$

□

Proof of Theorem 4. For any π, s, a , the value error is bounded by

$$\left| Q^\pi(s, a) - \phi_s^\top \mathbf{q}_\phi^a \right| = \left| r(s, a) + \gamma \mathbb{E}_{s'} \left[V^\pi(s') |s, a\right] - \phi_s^\top \mathbf{r}_\phi^a + \gamma \phi_s^\top \mathbf{P}_\phi^a \mathbf{v}_\phi^\pi \right| \quad (110)$$

$$\leq \left| r(s, a) - \phi_s^\top \mathbf{r}_\phi^a \right| + \gamma \left| \mathbb{E}_{s'} \left[V^\pi(s') |s, a\right] - \phi_s^\top \mathbf{P}_\phi^a \mathbf{v}_\phi^\pi \right| \quad (111)$$

The second transition error term can be upper bounded with

$$\left| \mathbb{E}_{s'} [V^{\bar{\pi}}(s') | s, a] - \boldsymbol{\phi}^\top \mathbf{P}_\phi^a \mathbf{v}^{\bar{\pi}} \right| \quad (112)$$

$$= \left| \mathbb{E}_{s'} [V^{\bar{\pi}}(s') | s, a] - \mathbb{E}_{s'} [\boldsymbol{\phi}_{s'}^\top \mathbf{v}^{\bar{\pi}} | s, a] + \mathbb{E}_{s'} [\boldsymbol{\phi}_{s'}^\top \mathbf{v}^{\bar{\pi}} | s, a] - \boldsymbol{\phi}^\top \mathbf{P}_\phi^a \mathbf{v}^{\bar{\pi}} \right| \quad (113)$$

$$\leq \max_s \left| V^{\bar{\pi}}(s) - \boldsymbol{\phi}_s^\top \mathbf{v}^{\bar{\pi}} \right| + \left\| \mathbb{E}_{s'} [\boldsymbol{\phi}_{s'}^\top | s, a] - \boldsymbol{\phi}^\top \mathbf{P}_\phi^a \right\|_2 \|\mathbf{v}^{\bar{\pi}}\|_2 \quad (114)$$

$$\leq \max_s \left| V^{\bar{\pi}}(s) - \boldsymbol{\phi}_s^\top \mathbf{v}^{\bar{\pi}} \right| + \varepsilon_\psi \frac{1 + \gamma}{\gamma(1 - \gamma)} \max_a \|\mathbf{r}_\phi^a\|_2 \quad (115)$$

Substituting Eq. (115) into Eq. (111) gives

$$\left| Q^\pi(s, a) - \boldsymbol{\phi}_s^\top \mathbf{q}_\phi^a \right| \leq \left| r(s, a) - \boldsymbol{\phi}_s^\top \mathbf{r}_\phi^a \right| + \gamma \left| \mathbb{E}_{s'} [V^{\bar{\pi}}(s') | s, a] - \boldsymbol{\phi}^\top \mathbf{P}_\phi^a \mathbf{v}^{\bar{\pi}} \right| \quad (116)$$

$$\leq \varepsilon_r + \gamma \max_s \left| V^{\bar{\pi}}(s) - \boldsymbol{\phi}_s^\top \mathbf{v}^{\bar{\pi}} \right| + \frac{\varepsilon_\psi(1 + \gamma)}{1 - \gamma} \max_a \|\mathbf{r}_\phi^a\|_2. \quad (117)$$

To complete the proof, note that the bound Eq. (117) was derived for any state s and action a . Hence

$$\forall s, a, \left| Q^\pi(s, a) - \boldsymbol{\phi}_s^\top \mathbf{q}_\phi^a \right| \leq B \implies \max_s \left| V^{\bar{\pi}}(s) - \boldsymbol{\phi}_s^\top \mathbf{v}^{\bar{\pi}} \right| \leq B, \quad (118)$$

because the bound B also holds for the maximizing state s and for deterministic and for stochastic $\bar{\pi}$ the bound holds as well, because $\bar{\pi}$ maps to an action. Hence

$$\left| Q^\pi(s, a) - \boldsymbol{\phi}_s^\top \mathbf{q}_\phi^a \right| \leq B = \varepsilon_r + \gamma \max_s \left| V^{\bar{\pi}}(s) - \boldsymbol{\phi}_s^\top \mathbf{v}^{\bar{\pi}} \right| + \frac{\varepsilon_\psi(1 + \gamma)}{(1 - \gamma)^2} \max_a \|\mathbf{r}_\phi^a\|_2 \quad (119)$$

$$\leq \varepsilon_r + \gamma B + \frac{\varepsilon_\psi(1 + \gamma)}{(1 - \gamma)^2} \max_a \|\mathbf{r}_\phi^a\|_2 \quad (120)$$

$$\iff \left| Q^\pi(s, a) - \boldsymbol{\phi}_s^\top \mathbf{q}_\phi^a \right| \leq \frac{\varepsilon_r}{1 - \gamma} + \frac{\varepsilon_\psi(1 + \gamma)}{(1 - \gamma)^2} \max_a \|\mathbf{r}_\phi^a\|_2. \quad (121)$$

□

Appendix B. Hyper Parameter for Experiments

Table 1 lists all hyper-parameters for the column world experiment, and Table 2 lists all hyper-parameters for the puddle world experiment.

Hyper-Parameter	Setting or Value
Gradient Optimizer	Adam Kingma and Ba (2014)
Learning Rate	0.02
Initialization	Uniform from $[0, 1]$
Number of features	3
α (Eq. (52) or Eq. (55))	0.01

Table 1: Column grid world experiment (Figure 1)

Hyper-Parameter	Setting or Value
Gradient Optimizer	Adam Kingma and Ba (2014)
Learning Rate	0.001
Initialization	Uniform from $[0, 1]$
Number of features	80
α (Eq. (52) or Eq. (56))	1.0
Batch Size	50

Table 2: Puddle World Experiment (Figure 4)

References

- David Abel, D Ellis Hershkowitz, and Michael L Littman. Near optimal behavior via approximate state abstraction. *arXiv preprint arXiv:1701.04113*, 2017.
- David Abel, Dilip Arumugam, Lucas Lehnert, and Michael Littman. State abstractions for lifelong reinforcement learning. In Jennifer Dy and Andreas Krause, editors, *Proceedings of the 35th International Conference on Machine Learning*, volume 80 of *Proceedings of Machine Learning Research*, pages 10–19, Stockholmsmässan, Stockholm Sweden, 10–15 Jul 2018. PMLR. URL <http://proceedings.mlr.press/v80/abel18a.html>.
- Kavosh Asadi, Dipendra Misra, and Michael Littman. Lipschitz continuity in model-based reinforcement learning. In Jennifer Dy and Andreas Krause, editors, *Proceedings of the 35th International Conference on Machine Learning*, volume 80 of *Proceedings of Machine Learning Research*, pages 264–273, Stockholmsmässan, Stockholm Sweden, 10–15 Jul 2018. PMLR. URL <http://proceedings.mlr.press/v80/asadi18a.html>.
- André Barreto, Will Dabney, Rémi Munos, Jonathan J Hunt, Tom Schaul, Hado P van Hasselt, and David Silver. Successor features for transfer in reinforcement learning. In *Advances in neural information processing systems*, pages 4055–4065, 2017.
- Andre Barreto, Diana Borsa, John Quan, Tom Schaul, David Silver, Matteo Hessel, Daniel Mankowitz, Augustin Zidek, and Remi Munos. Transfer in deep reinforcement learning using successor features and generalised policy improvement. In Jennifer Dy and Andreas Krause, editors, *Proceedings of the 35th International Conference on Machine Learning*, volume 80 of *Proceedings of Machine Learning Research*, pages 501–510, Stockholmsmässan, Stockholm Sweden, 10–15 Jul 2018. PMLR. URL <http://proceedings.mlr.press/v80/barreto18a.html>.
- Marc G. Bellemare, Yavar Naddaf, Joel Veness, and Michael Bowling. The arcade learning environment: An evaluation platform for general agents. *CoRR*, abs/1207.4708, 2012. URL <http://arxiv.org/abs/1207.4708>.
- Christopher M. Bishop. *PATTERN RECOGNITION AND MACHINE LEARNING*. Springer-Verlag New York, 2006.
- Justin A Boyan. Least-squares temporal difference learning. In *ICML*, pages 49–56, 1999.

- Justin A Boyan and Andrew W Moore. Generalization in reinforcement learning: Safely approximating the value function. In *Advances in neural information processing systems*, pages 369–376, 1995.
- Ronen I Brafman and Moshe Tennenholtz. R-max-a general polynomial time algorithm for near-optimal reinforcement learning. *Journal of Machine Learning Research*, 3(Oct): 213–231, 2002.
- Peter Dayan. Improving generalization for temporal difference learning: The successor representation. *Neural Computation*, 5(4):613–624, 1993.
- Eyal Even-Dar and Yishay Mansour. Approximate equivalence of markov decision processes. In *Learning Theory and Kernel Machines*, pages 581–594. Springer, 2003.
- Norm Ferns, Prakash Panangaden, and Doina Precup. Metrics for finite markov decision processes. In *Proceedings of the 20th conference on Uncertainty in artificial intelligence*, pages 162–169. AUAI Press, 2004.
- Norm Ferns, Prakash Panangaden, and Doina Precup. Bisimulation metrics for continuous markov decision processes. *SIAM Journal on Computing*, 40(6):1662–1714, 2011.
- Chelsea Finn, Xin Yu Tan, Yan Duan, Trevor Darrell, Sergey Levine, and Pieter Abbeel. Learning visual feature spaces for robotic manipulation with deep spatial autoencoders. *CoRR*, abs/1509.06113, 2015. URL <http://arxiv.org/abs/1509.06113>.
- Robert Givan, Thomas Dean, and Matthew Greig. Equivalence notions and model minimization in markov decision processes. *Artificial Intelligence*, 147(1):163–223, 2003.
- David Ha and Jürgen Schmidhuber. World models. *arXiv preprint arXiv:1803.10122*, 2018.
- Leslie Pack Kaelbling, Michael L Littman, and Andrew W Moore. Reinforcement learning: A survey. *Journal of artificial intelligence research*, 4:237–285, 1996.
- Diederik P. Kingma and Jimmy Ba. Adam: A method for stochastic optimization. *CoRR*, abs/1412.6980, 2014. URL <http://arxiv.org/abs/1412.6980>.
- George Konidaris, Sarah Osentoski, and Philip Thomas. Value function approximation in reinforcement learning using the fourier basis. *Proceedings of the Twenty-Fifth AAAI Conference on Artificial Intelligence*, pages 380–385, August 2011.
- Tejas D Kulkarni, Ardavan Saeedi, Simanta Gautam, and Samuel J Gershman. Deep successor reinforcement learning. *arXiv preprint arXiv:1606.02396*, 2016.
- Lucas Lehnert, Stefanie Tellex, and Michael L Littman. Advantages and limitations of using successor features for transfer in reinforcement learning. *arXiv preprint arXiv:1708.00102*, 2017.
- Lucas Lehnert, Romain Laroche, and Harm van Seijen. On value function representation of long horizon problems. *Proceedings of the Thirty-Second AAAI Conference on Artificial Intelligence*, 2018. URL <https://www.aaai.org/ocs/index.php/AAAI/AAAI18/paper/view/16388>.

- Lihong Li, Thomas J Walsh, and Michael L Littman. Towards a unified theory of state abstraction for mdps. In *ISAIM*, 2006.
- Volodymyr Mnih, Koray Kavukcuoglu, David Silver, Alex Graves, Ioannis Antonoglou, Daan Wierstra, and Martin A. Riedmiller. Playing atari with deep reinforcement learning. *CoRR*, abs/1312.5602, 2013. URL <http://arxiv.org/abs/1312.5602>.
- Volodymyr Mnih, Koray Kavukcuoglu, David Silver, Andrei A Rusu, Joel Veness, Marc G Bellemare, Alex Graves, Martin Riedmiller, Andreas K Fidjeland, Georg Ostrovski, et al. Human-level control through deep reinforcement learning. *Nature*, 518(7540):529–533, 2015.
- Ida Momennejad, Evan M Russek, Jin H Cheong, Matthew M Botvinick, ND Daw, and Samuel J Gershman. The successor representation in human reinforcement learning. *Nature Human Behaviour*, 1(9):680, 2017.
- Junhyuk Oh, Satinder Singh, and Honglak Lee. Value prediction network. *arXiv preprint arXiv:1707.03497*, 2017.
- Ronald Parr, Lihong Li, Gavin Taylor, Christopher Painter-Wakefield, and Michael L Littman. An analysis of linear models, linear value-function approximation, and feature selection for reinforcement learning. In *Proceedings of the 25th international conference on Machine learning*, pages 752–759. ACM, 2008.
- Martin L Puterman. *Markov decision processes: discrete stochastic dynamic programming*. John Wiley & Sons, 1994.
- Sherry Shanshan Ruan, Gheorghe Comanici, Prakash Panangaden, and Doina Precup. Representation discovery for mdps using bisimulation metrics. In *AAAI*, pages 3578–3584, 2015.
- Gavin Adrian Rummery. *Problem Solving with Reinforcement Learning*. PhD thesis, Cambridge University Engineering Department, Trumpington Street, Cambridge, CD2 1PZ, England, 1995.
- Evan M Russek, Ida Momennejad, Matthew M Botvinick, Samuel J Gershman, and Nathaniel D Daw. Predictive representations can link model-based reinforcement learning to model-free mechanisms. *PLoS computational biology*, 13(9):e1005768, 2017.
- Zhao Song, Ronald E Parr, Xuejun Liao, and Lawrence Carin. Linear feature encoding for reinforcement learning. In *Advances in Neural Information Processing Systems*, pages 4224–4232, 2016.
- Alexander L Strehl, Lihong Li, Eric Wiewiora, John Langford, and Michael L Littman. Pac model-free reinforcement learning. In *Proceedings of the 23rd international conference on Machine learning*, pages 881–888. ACM, 2006.
- Alexander L Strehl, Lihong Li, and Michael L Littman. Reinforcement learning in finite mdps: Pac analysis. *Journal of Machine Learning Research*, 10(Nov):2413–2444, 2009.

- Richard S. Sutton. Learning to Predict by the Methods of Temporal Differences. *Machine Learning*, 3(1):9–44, August 1988.
- Richard S Sutton. Integrated architectures for learning, planning, and reacting based on approximating dynamic programming. In *Proceedings of the seventh international conference on machine learning*, pages 216–224, 1990.
- Richard S Sutton. Generalization in reinforcement learning: Successful examples using sparse coarse coding. *Advances in neural information processing systems*, pages 1038–1044, 1996.
- Richard S. Sutton and Andrew G. Barto. *Reinforcement Learning: An Introduction*. A Bradford Book. MIT Press, Cambridge, MA, 1 edition, 1998.
- Richard S. Sutton, Csaba Szepesvári, Alborz Geramifard, and Michael Bowling. Dyna-style planning with linear function approximation and prioritized sweeping. In *Proceedings of the 24th Conference on Uncertainty in Artificial Intelligence*, 2008.
- Erik Talvitie. Self-correcting models for model-based reinforcement learning. In *AAAI*, pages 2597–2603, 2017.
- Erik Talvitie. Learning the reward function for a misspecified model. In Jennifer Dy and Andreas Krause, editors, *Proceedings of the 35th International Conference on Machine Learning*, volume 80 of *Proceedings of Machine Learning Research*, pages 4838–4847, Stockholmsmässan, Stockholm Sweden, 10–15 Jul 2018. PMLR. URL <http://proceedings.mlr.press/v80/talvitie18a.html>.
- Christopher J.C.H. Watkins and Peter Dayan. *Q-learning*. *Machine Learning*, 8(3):279–292, May 1992.
- Théophane Weber, Sébastien Racanière, David P Reichert, Lars Buesing, Arthur Guez, Danilo Jimenez Rezende, Adria Puigdomènech Badia, Oriol Vinyals, Nicolas Heess, Yujia Li, et al. Imagination-augmented agents for deep reinforcement learning. *arXiv preprint arXiv:1707.06203*, 2017.
- Hengshuai Yao and Csaba Szepesvári. Approximate policy iteration with linear action models. In *AAAI*, 2012.
- Jingwei Zhang, Jost Tobias Springenberg, Joschka Boedecker, and Wolfram Burgard. Deep reinforcement learning with successor features for navigation across similar environments. *arXiv preprint arXiv:1612.05533*, 2016.